



Babeş-Bolyai University of Cluj-Napoca
Faculty of Physics
Biomolecular Physics Department



**Raman Spectroscopy Techniques and Applications to
Carotenoids Research in Marine Living Resources and to
the Blue Bioeconomy**

Doctoral Thesis summary

by:

Fran Nekvapil

Scientific supervisor:

Prof. Dr. habil. Simona Cintă Pinzaru

Cluj-Napoca, 2020

Content (refers to *in extenso* Thesis):

Acknowledgements	1
1. General Introduction	2
1.1. Structure and purpose of this Thesis	2
1.2. Raman spectroscopy: technology and methodology	4
1.3. Carotenoids: physical and chemical properties	4
1.4. Widening the field of applications: Raman spectroscopy techniques for marine environment and its resources	5
1.5. Raman techniques employed and general characteristics of the instruments used in the presented research	6
2. Experimental aspects of Raman spectroscopy investigation of carotenoids in native fruits biomatrix: the case of citrus varieties and their peel	6
2.1. Citrus fruits freshness assessment using Raman spectroscopy - original research article	6
3. Carotenoid Raman signal behaviour and electronic structure described by multi-laser (micro) Raman and DFT; carotenoid signal as a physiology marker in cyanobacteria probed by <i>in vivo</i> single-cell Resonance Raman	8
3.1. Comprehensive description of Raman spectra and electronic structure of fucoxanthin	8
3.2. Non-resonance excitation of solid-state fucoxanthin and β -carotene: differentiation of carotenoids in complex biosystems	11
3.3. Effect of metallic nanoparticles aggression on the carotenoid Raman signal of cyanobacteria on cellular level	13
3.4. Manganese zinc ferrite nanoparticles and their Raman spectroscopy - original research article	15
3.5. Chapter 3 conclusions	15
4. Comparative tissue analysis, <i>in situ</i> detection and biochemical roles of carotenoids studied by Resonance Raman and SERS; delicate tissue preparation and preservation for Raman analysis	16
4.1. Comparative study of carotenoid metabolism in sea urchins studied by Resonance Raman spectroscopy and SERS techniques	17
4.1.1. Carotenoids detection and characterization in echinoderms	17
4.1.2. General sampling procedures	17
4.1.3. SERS detection of carotenoids in the digestive system extracts	18
4.1.4. SERS detection of carotenoids in the coelomic fluid	18
4.1.5. Echinenone and β -carotene of sea urchin gonads - effect of molecular environment on the carotenoid Raman bands	18
4.1.6. Resonance micro-Raman detection of carotenoids in native sea urchin eggs	19
4.1.7. Resonance micro- Raman localization of the carotenoid signal in larvae	19
4.2. Comparative Raman spectroscopy study of the coelomic fluid of grazing sea urchins and their native seawater: prospect for a potential indicator of environmental aggression - full length conference contribution	20
4.3. Microsphere packages of carotenoids: intact sea urchin eggs tracked	21

by Paman spectroscopy tools - original research article	
4.4. Exploring the biological protective role of carotenoids by Raman spectroscopy: mechanical stress of cells-original research article	22
4.5. Chapter 4 conclusions	23
5. Change of optical properties of carotenoids upon binding to proteins crustacyanins investigated by Resonance Raman with multiple laser lines and by DFT; similarities of their signal to unsaturated polyenes; application of Raman spectroscopy in Blue bioeconomy and Circular economy	24
5.1. Resonance Raman signal of crustacean pigments located in a porous biogenic carbonate structures - controversies and new breakthroughs on the origin of colour	25
5.2. Natural nanoarchitecture of Blue crab (<i>Callinectes sapidus</i> Rathbun, 1896) claw studied by Raman spectroscopy and scanning electron microscopy	27
5.3. Color-specific porosity in double pigmented natural 3d-nanoarchitectures of blue crab shell - original research article	28
5.4. From Blue bioeconomy toward Circular economy through high-sensitivity analytical research on waste Blue crab shells - original research article	29
5.5. Promoting hidden natural design templates in wasted shells of the mantis shrimp into valuable biogenic composite	29
5.7. Chapter 5 references	195
6. Conclusions, impact and perspectives	31
Selected references	33
Abbreviations	36
List of publications included in the Thesis	36
Summary	38

Acknowledgements

First and foremost, I wish to express my deepest thanks to Prof. habil. dr. Simona Cintă Pinzaru, my guide through the realm of science. Her leadership enhanced my professional development and spilled over to many spheres of my private life. If I had to choose a single, most important lesson I learned from her, it has to be that I'm capable of taking on any challenge, no matter how bad the odds may be; there is no such thing as *not being good enough*. I have learned to value my work and not to give up before the battle has even started.

Prof. dr. Vasile Chiş is credited with high-quality computational chemistry results which notably enriched the studies presented in this Thesis. I wish to express my great thanks his guidance and support.

Conf. dr. Lucian Barbu-Tudoran is credited for the insightful electron microscopy results and discussion throughout the studies comprised in this Thesis. I also acknowledge his effort with the highest regards.

My Guidance Committee, comprising Prof. dr. Vasile Chiş, Conf dr. Lucian Barbu-Tudoran and Prof. dr. Horia Banciu, provided very constructive suggestions which streamlined this document and made the Thesis more clear and impactful. Furthermore, dr. Sanja Tomšič and dr. Branko Glamuzina provided invaluable help in samples collection and preparation.

Also, I wish to thank numerous other researchers from the Babeş-Bolyai University, the University of Dubrovnik, and the National Institute for Research and Development of Isotopic and Molecular Technologies in Cluj-Napoca, who provided valuable assistance or discussions during my doctoral programme.

I wish to acknowledge my family, which supported me in various ways, but primarily with love and understanding. I will now also remember my dear friends, who shone a spark of light even in my dim days and continually lifted up my spirits.

The realization of this Thesis would not be possible without the infrastructure, facilities and grants of the Babeş-Bolyai University, renowned for its tradition and excellence. This support is acknowledged with highest regards.

The University of Dubrovnik is credited for my initiation in the cross-border work, and welcoming provision of research facilities. More precisely, my participation in the Erasmus+ programme (financed by the European Union) to Babeş-Bolyai University, granted during my study at the University of Dubrovnik motivated the work presented on the following pages.

The National Institute for Research and Development of Isotopic and Molecular Technologies (INCDTIM Cluj-Napoca), its personnel and facilities are also acknowledged for enriching this Thesis with additional experimental possibilities and inputs.

1. GENERAL INTRODUCTION

1.1. Structure and purpose of this Thesis

In 1921, the Indian scientist Sir Chandrasekhara Venkata Raman was on a voyage to Europe, where he was fascinated by the blue colour of the Mediterranean Sea, which inspired further experimental work and yielded a proof of a new optical process several years later. In fact, his 1930 Nobel Prize lecture opened with the clause “*The colour of the sea*” (Raman, 1930). A Web of Science database search (www.webofknowledge.com) for terms “Raman” + “marine” shows that Raman spectroscopy application related to the marine environment gained momentum around 2013 (Figure 1), but the research began much earlier: the *in vivo* recording of Raman signal of carotenoid pigments in live lobster carapace as early as 1977 (Salares et al., 1977) represents a clever use of Resonance Raman spectroscopy, a technique which is also used throughout the work described in this Thesis. However, it was only since two decades ago, that the Raman spectrometer systems technology became mature, robust and compact enough to enable *in situ* measurements of the environmental processes deep under the sea surface (Pasteris et al., 2004; Zhang et al., 2012).

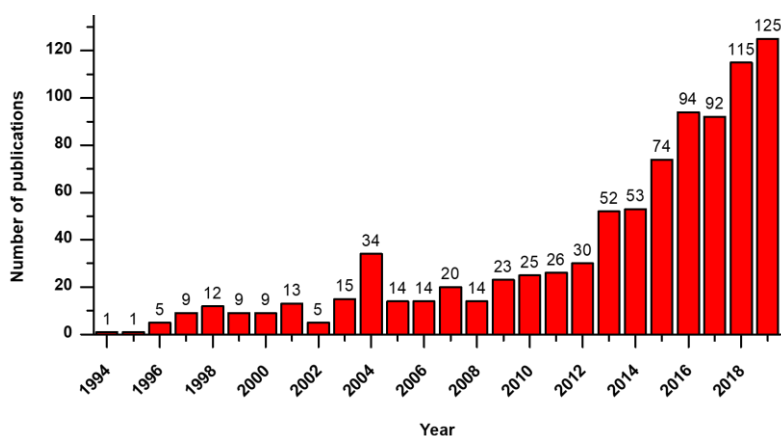


Figure 1. Plot of number of publications including the words “Raman” + “marine” versus the publication years, obtained through the *search* tool of the Web of Science platform (www.webofknowledge.com). The Figure displays the year range from 1994 and 2019, where the continuity of publications was observed. Due to the limited search parameters, the plot may not represent the full range of employment of Raman spectroscopy in the period; however, the increasing trend and interest in application of Raman spectroscopy techniques to marine environment research is clear.

The concepts of Blue bioeconomy, the most efficient exploitation of marine resources without degrading their capacity for renewal are appealing; however, a lot of further work is needed to answer the question of “how to actually achieve those

concepts?” This also includes the sub-question of “how to effectively characterize the material at hand, but without excessive sample preparation and consumption of chemicals, labour and time?”

The main goal of the here presented Doctoral thesis the extension of the applicability of experimental and theoretical Raman spectroscopy techniques, including RRS, SERS, SERRS, NIR-Raman, FT-Raman, and DFT, in marine biology and biophysics studies. The Thesis is further aimed demonstrating high-precision molecular detection of carotenoids in native, real-world complex biological samples, rather than remaining in the confinements of the laboratory setups and standard compounds. Hence, the findings and the methodology improvements can indeed address the above discussed concepts and questions. Hence, the work presented here opens hitherto unexploited opportunities to tackle the major biological, biotechnological and economic issues related to marine environment from a new point of view.

The research presented here followed four main lines of experiments, grouped by the samples type in four Chapters. All of the conducted studies feed into the common aim: gain better understanding of the carotenoid (and carotenoprotein) Raman signal and extend the applicability of experimental Raman techniques and computational chemistry methods to the marine biotechnology and its attached fields. We further address and present our views on the major controversies regarding the Raman signal of these pigments, and present our contributions to unravelling some of the long-standing discussions in the scientific community. Figure 2. displays schematically the superstructure of this Thesis.

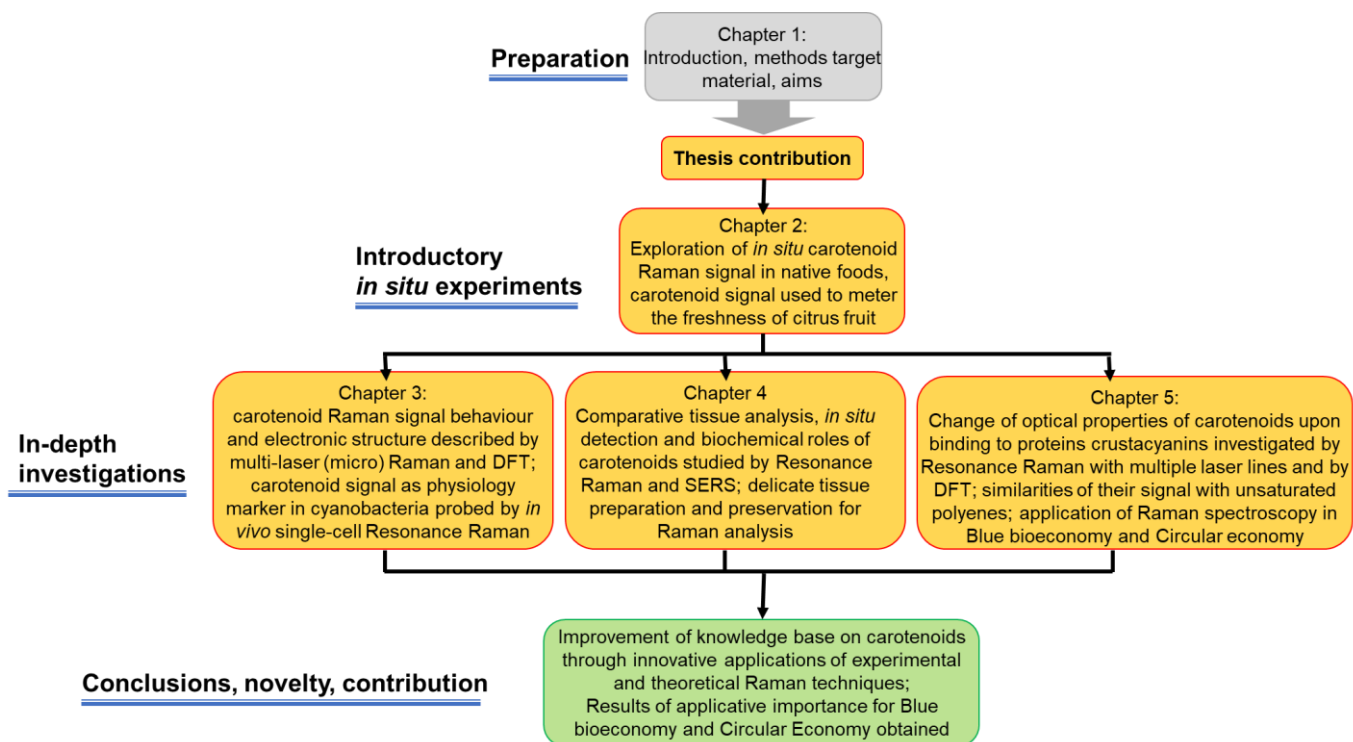


Figure 2. Schematic display of the superstructure and flow of this Thesis.

1.2. Raman spectroscopy: technology and methodology

The introductory sections of a book by Ewen Smith and Geoffrey Dent titled “Modern Raman spectroscopy - A practical approach”, summarize the basics of Raman spectroscopy analysis in a manner easy to read and understand (Smith and Dent, 2005). Briefly, inelastic (Raman) scattering occurs when the incident photons cause nuclear motion, which subsequently changes the energy of the scattered photon. This energy difference is the basis of a Raman spectroscopy (RS) measurement. Both Raman spectroscopy and the widely used infrared absorption spectroscopy (IR) are methods for probing the molecular structure of the sample according to photons interaction with the atomic bonds (scattering in RS and absorption in IR). Raman spectroscopy, however, exhibits greater performance in analysis of hydrated samples due to the relatively lower scattering cross-section of the O-H bonds, which is advantageous for probing of native biological and environmental samples.

1.3. Carotenoids: physical and chemical properties

The introduction to the carotenoids, as the molecular targets of the studies described herein, is due. According to Maoka (2020), near 1000 carotenoid structures have been hitherto described, with many of them found only in specific organisms. However, only about 40 carotenoids appear in a typical human diet. These common carotenoids are usually obtained through fruit and vegetables. These compounds have attracted attention of the scientific community due to their association with photosynthesis and energy capture and transfer, e.g. fucoxanthin in diatoms (Gundermann and Büchel, 2014), β -carotene, violaxanthin, 9'-*cis*-neoxanthin and lutein in green algae (Takaichi, 2011), α -carotene, β -carotene, zeaxanthin and lutein in red algae (Takaichi, 2011), and a wider range of carotenoids in higher plants. Furthermore, provitamin A derivation (most notably from β -carotene; Tang 2010) and overall beneficial effects to the living organisms (Dose et al., 2016) is another important attribute of carotenoids. Certain carotenoids, like lutein and zeaxanthin are critical for normal function of the eye retina in mammals (Widjaja-Adhi et al., 2018). The common carotenoids have a terpenoid structure (Sections 3.1. and 3.2.), and their biological roles are primarily mediated through the free radical scavenging capacity (Mortensen and Skibsted, 1997) and the UV-Vis absorption in 200 - 300 nm (lower) and 400 - 500 nm (higher) range (Flores-Hidalgo et al., 2017). The nature also exploits deposited and aggregated carotenoids, being yellowish, red, or brownish in colour, as a vivid colorant for invertebrate shells (Figure 3.) Furthermore, an indirect protective role of carotenoids against oxidative stress was shown in mouse model, where food supplementation with canthaxanthin promoted higher activity of antioxidant enzymes in the skin (Andrei et al., 2007). A detailed account on carotenoids is given in the book by John T. Landrum and others, titled “*Chemistry and Biochemistry of Carotenoids*” (Landrum et al., 2010).

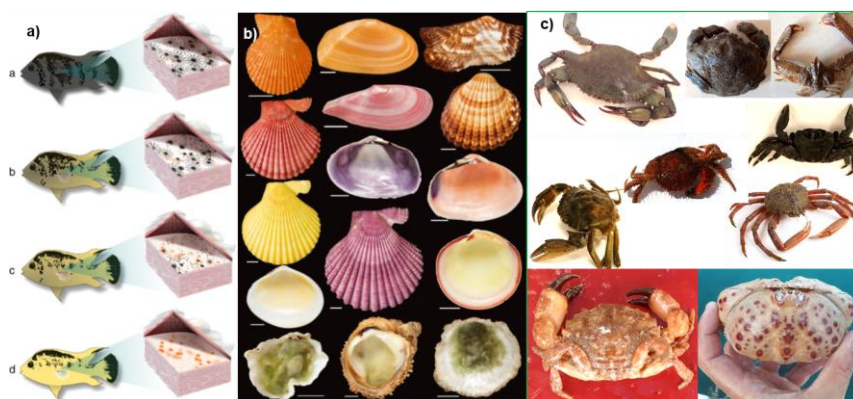


Figure 3. The diversity of shell coloration in aquatic animals based on carotenoids and unsaturated polyenes: a) male tilapias (reproduced from Sefc et al., 2014, licensed under Creative Commons CC-BY Attribution); b) bivalve mollusc shells (reproduced from Wade et al., 2019, by the permission of Wiley and Sons, licence no. 4864300984502); c) crustacean shells (Section 5.1.; photo credits: Fran Nekvapil, Branko Glamuzina, Ana Gavrilović). For more details, see the respective publications/section.

1.4. Widening the field of applications: Raman spectroscopy techniques for marine environment and its resources

This section is composed as a brief survey of the fields in marine biology, biochemistry and ecology research where Raman spectroscopy techniques show a unique appeal, due to the non-destructive and rapid character of the analysis, coupled with high sensitivity to molecular structure and high degree of spatial resolution. In some cases there is even no suitable alternative research or monitoring method. The current Thesis follows this tracks and enhances the utility of Raman spectroscopy in current fields and extends its range of applications. An exhaustive literature review is not attempted here, but rather, the following sections outline the frame of the present study by placing Raman spectroscopy techniques within the context of economy, environmental and social issues (Figure 4.).

Application area	Impact components			
	Scientific	Economic	Environmental	Social
Carotenoids	█	█		
Pollution			█	█
Seafood		█		█
Marine toxins	█	█	█	█
Deep sea	█	█	█	
Biocalcification	█	█	█	
Archaeology	█			█
Blue bioeconomy	█	█	█	█

Figure 4. Preview of main application areas of Raman spectroscopy related to marine biology and their impact components.

1.5. Raman techniques employed and general characteristics of the instruments used in the presented research

This Section describes the instruments, their advantages and disadvantages, and the techniques for which the particular instruments are suitable. Further sections of this Thesis will give specific details on respective sample analysis setup, however, reference will be made to the general device properties outlined here in order to avoid repetitions.

All experiments (Chapter 2 - Chapter 5) are characterized by the use of either of, or both, Resonance Raman spectroscopy (RRS) or Surface-enhanced Raman scattering (SERS). Where feasible, the RRS results were compared against non-resonant spectra acquired with NIR laser lines (785 or 1064 nm) and the Density Functional Theory (DFT) calculations and band assignments. Supporting and complementary results were also obtained by FT-Raman spectroscopy and electron microscopy, where appropriate.

2. EXPERIMENTAL ASPECTS OF RAMAN SPECTROSCOPY INVESTIGATION OF CAROTENOIDS IN NATIVE FRUITS BIOMATRIX: THE CASE OF CITRUS VARIETIES AND THEIR PEEL

2.1. Citrus fruits freshness assessment using Raman spectroscopy – original research article

Chapter 2 aims to present the detection of the carotenoid Raman signal in the real-world samples; in this case we considered the citrus fruits, which require no prior sample preparation to achieve the *in situ* Raman analysis in the peel. The study deals with a coastal human food chain, and presents important experimental aspects of carotenoids analysis in human day-to-day food.

A considerable number of published studies aimed to develop indicators for fruit and vegetable freshness or ripening stage, considering mostly the signal of lycopene and β -carotene in tomatoes (e.g. Martin et al., 2017; Hara et al., 2018 and references therein), but also in other foods (). Hence, there is little doubt that the 3 main bands of carotenoids [$\nu_1(\text{C}=\text{C})$, $\nu_2(\text{C}-\text{C})$ and $\nu_3(\text{C}-\text{CH}_3)$] can easily be recorded. However, certain authors (Jehlička et al., 2014; de Oliveira et al., 2010; Schulz et al., 2005; Oren et al., 2015).

However, this Chapter, as well as all of the following Sections of this document, demonstrates that carotenoid differentiation either in resonant or non-resonant signal, can be achieved by increasing the level of spectral analysis. This means, depending on the particular case, band width (FWHM) consideration, band

envelope deconvolution, direct band comparison between spectra of corresponding samples, or illuminating the same spot with multiple laser lines resonant to different pigments.

Additionally, in the following study (Section 2.1.), we propose a simple model for *in situ* assessment of freshness state of citrus fruit taking advantage of the carotenoid Raman signal intensity and the information contained in the level of spectral background. Carotenoids inherently exhibit a certain low, incremental fluorescence background under the 532 nm excitation, arising from their $S_1 \rightarrow S_0$ decay with low fluorescence yield (Noguchi et al., 1989; Kukura et al., 2004; Redeckas et al., 2016). Other chemical components with non-specific Raman signal also contribute to the spectral background, and the systematic increase of the spectral background through time, coupled with the simultaneous decrease of overall Raman signal of carotenoids, allowed us to define the *coefficient of freshness* expressed as $C_{\text{fresh}} = I_{\text{Raman signal}} / I_{\text{Raman background}}$ at the $\nu_1(\text{C}=\text{C})$ band. This spectra interpretation framework works both on lab-based and on portable Raman instruments, enabling perspective on site freshness determination.

This study was:

- *published in Food Chemistry, on 1. March 2018, Impact factor (2018) = 5.39;*
 - Citation: Nekvapil, F., Brezestean, I., Barchewitz, D., Glamuzina, B., Chis, V., Cintă Pinzaru, S. Citrus fruits freshness assessment using Raman spectroscopy. Food Chem. 2018a, 242: 560–567. DOI: 10.1016/j.foodchem.2017.09.105.
- *presented orally at the 16th International Symposium Prospects for the 3rd Millennium Agriculture, Cluj-Napoca (Romania), 28th – 30th September 2018*
 - Citation: Nekvapil, F., Brezestean, I., Barchewitz, D., Glamuzina, B., Chis, V., Cintă Pinzaru, S., Andronie, L. Are the market citrus fresh? Raman spectroscopy can promptly tell it. In: Vodnar, D.C. (ed.) Book of Abstracts, no. 4/2017. Faculty of Agricultural Sciences and Veterinary Medicine of Cluj-Napoca, ISSN: 2392-6937, ISSN-L: 2392-6937. p. 230.

3. CAROTENOID RAMAN SIGNAL BEHAVIOUR AND ELECTRONIC STRUCTURE DESCRIBED BY MULTI-LASER (MICRO) RAMAN AND DFT; CAROTENOID SIGNAL AS A PHYSIOLOGY MARKER IN CYANOBACTERIA PROBED BY *IN VIVO* SINGLE-CELL RESONANCE RAMAN

Despite the importance of fucoxanthin in biomedicine and pharmacology, this compound is still not comprehensively characterized by Raman spectroscopy techniques. This would allow its rapid detection, identification and quantification, and the overall increase in efficiency of its research. Sections 3.1. and 3.2. are aimed at detailed theoretical and experimental studies on the Raman signal of pure carotenoids fucoxanthin and β -carotene, including the consideration of major and minor bands and quantitative prospects, and with the focus on the structure of their strong $\nu_1(\text{C}=\text{C})$ band. To achieve this, we employed Resonance and non-resonance Raman excitation, DFT calculations, SERS and FT-Raman. Furthermore, we prospect the carotenoid *in situ* differentiation in unicellular photosynthetic microorganisms: fucoxanthin in diatoms *Cylindrotheca closterium* and *Skeletonema costatum*, and β -carotene in cyanobacteria *Coelomorion pussilum*. Thereafter, using the obtained knowledge, in the Section 3.3. we exploit the Resonance Raman signal from *C. pussilum* single cells exposed to ferrite nanoparticles to prospect the utility of microbial carotenoid signal in ecotoxicological studies.

3.1. Comprehensive description of Raman spectra and electronic structure of fucoxanthin

Raman spectra acquired from fucoxanthin polycrystalline powder, the stock solution in ethanol, and the highest concentration SERS solution are presented in Figure 5. All spectra featured the four major Raman bands, the ν_1 (1522 - 1531 cm^{-1}), ν_2 (1140 - 1200 cm^{-1}), ν_3 (1010 - 1020 cm^{-1}) and ν_4 (961 - 964 cm^{-1}), and several weaker bands which will be addressed in the following. Fucoxanthin was pre-resonantly excited with 532 nm, as observed by the presence of overtones in 2000 to 3100 cm^{-1} region, and non-resonantly with 632.8 and 785 nm laser lines,. The positions and assignments of all observed bands are given in Table 1.

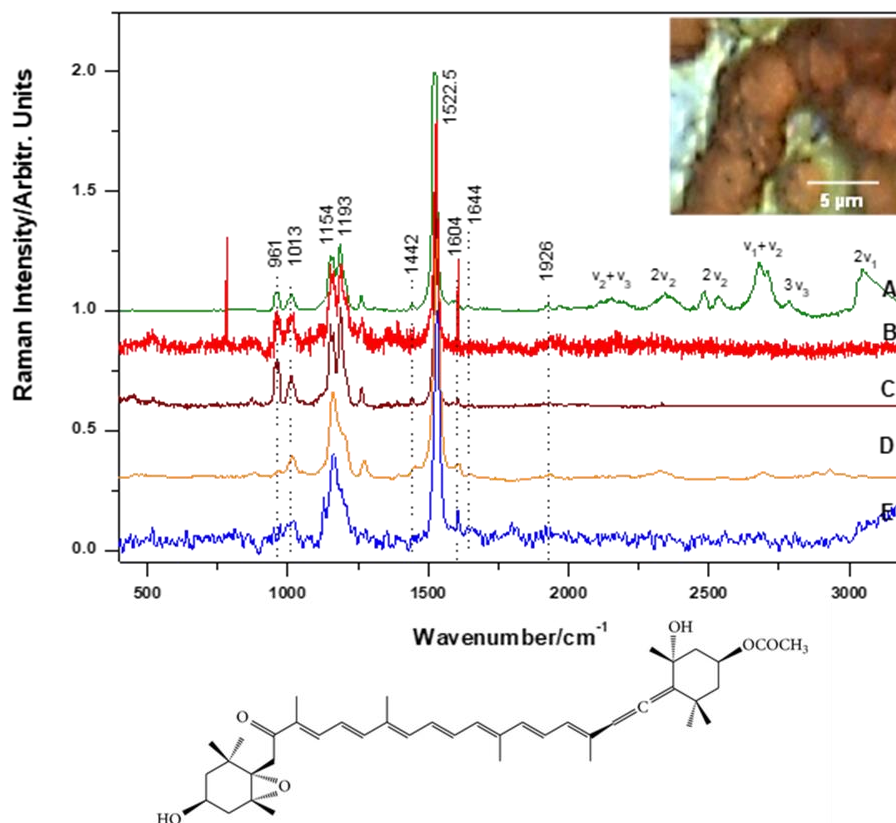


Figure 5. Raman spectra of fucoxanthin standard. (A-C) organic crystals under (A) 532 nm, (B) 632.8, and (C) 785 nm excitation. (D) 3.063 mmol l⁻¹ ethanol solution and (E) 12.008 μmol l⁻¹ SERS solution under 532 nm. Inset micrograph shows fucoxanthin organic crystals (100x). The scheme below presents the chemical structure of fucoxanthin. Band positions refer to spectrum (A).

The decay of Raman signal intensity of fucoxanthin dissolved in ethanol with decreasing concentration is shown in Figure 6a. The relative fucoxanthin signal, plotted as ratio between bands at 1531 cm⁻¹ (ν₁) and 2930 cm⁻¹ (ethanol), exhibits a linear trend over the tested concentration range, described by the function $y = 0.045 + 0.032x$.

The concentration-to-signal intensity relationship is presented in Figure 6b. The relationship between bands at 1527 cm⁻¹ (ν₁) and 3168 cm⁻¹ (water) is described by the intensity ratio $R = I_{1527} / I_{3168}$, and follows a 3rd order polynomial fit with the function $y = 2.91 + 0.12(x^1) + 1.137(x^2) + 0.545(x^3)$ across the tested concentration range. Interestingly, the intensity of bands at 1128 and 1606 cm⁻¹ did not exhibit a clear concentration dependency over the tested range of concentrations.

Table 1. Positions and assignments of the fucoxanthin Raman bands acquired under three excitation lines in various aggregation state, molecular environment and analysis technique (normal Raman, SERS, DFT, live *C. closterium*).

Experimental bands						Calculated mode	
org. cryst., 532 nm	org. cryst., 632.8 nm	org. cryst , 785 nm	EtOH solution, 532 nm	SERS modes, 532 nm	<i>C. closterium</i> Raman 532 nm	gaseous c1 scaled	Assignment
1929	1933	1933	1933			1949	$\nu_{as}(C=C=C)$
1644			1651		1653		$\nu(C8=O)$
1602	1608	1607	1609	1607	1610	1607	$\nu(C=C)$ out of phase
1585	1590	1590					$\nu(C=C)$ centre of polyene chain*
1522.5	1529	1529.5	1532	1531	1526, 1532 (sh)	1513	$\nu(C=C)$ in phase
1441		1445	1451	1448	1444	1444	$\delta_{as}(CH_3)$
1385	1390	1390	1393	1392			sym. $\delta(CH_3)^*$
1353	1355	1355	1358				$\rho(CH_3) + \text{sym } \delta(CH_3)^*$
1311							$\nu(C=C)$ centre of polyene chain*
1260	1262	1264	1271	1267		1263	$\nu(C-C)+\beta(CH)$
	1235			1236			$\rho(C-H)^*$
1202	1212 sh	1212 sh	1205	1209	1212	1256	$\tau(CH_2)$
1184	1188	1188	1183	1191		1173	$\nu(C-C)+\beta(CH)$
			1160	1163	1158	1161	$\nu(C-C)$ $+\delta(CCC)_{ring}$
1153	1155	1155				1154	$\nu(C-C)+\beta(CH)$
1089		1098	1110	1128			$\nu(C-C)$ cyclohexene ring*
1011	1010,1018	1010,1018 (sh)	1015	1010	1013	1023	$\delta(CCC)+\rho(CH_3)$
961	961	960	964	961	961	979	$\rho(CH_3)$

*assignments analogous to β -carotene from Cintă Pinzaru et al. (2015)

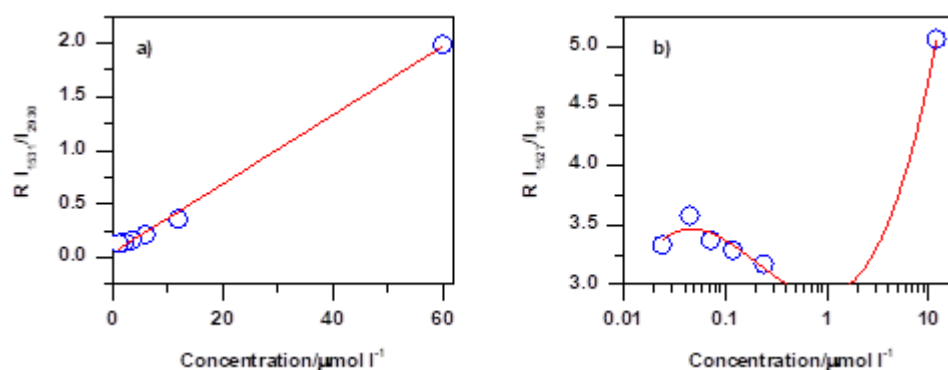


Figure 6. Plots of relative intensity of (a) fucoxanthin Raman band at 1531 cm^{-1} to ethanol $\nu(\text{C-H})$ mode at 2930 cm^{-1} , and (b) fucoxanthin SERS band (1527 cm^{-1}) to water band around 3168 cm^{-1} , showing the fucoxanthin signal intensity trend across micromolar concentrations. The x-axis in (b) are set to logarithmic scale for clarity. The Raman intensity decay is fitted by a linear fit ($y = 0.045 + 0.032x$), and SERS intensity with a 3rd order polynomial fit [$y = 2.91 + 0.12(x^1) + 1.137(x^2) + 0.545(x^3)$].

Raman spectra of fucoxanthin were also detected here *in vivo* from the diatom *Cylindrotheca closterium* (Figure 7)

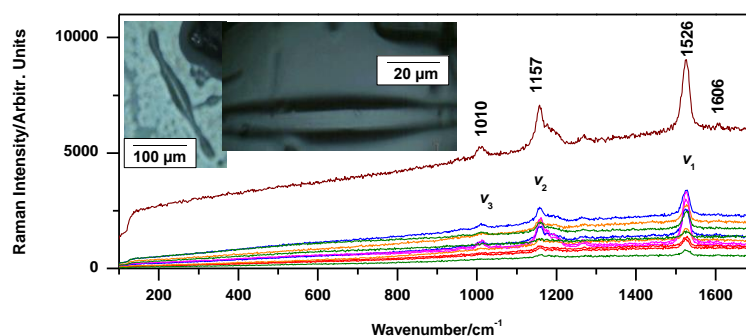


Figure 7. Unprocessed Raman spectra of *Cylindrotheca closterium* diatom green cell bodies, acquired under 532 nm excitation and shown in 150 - 1650 cm^{-1} range. Different colours refer to 6 different cells. Carotenoid ν_1 , ν_2 and ν_3 bands are labelled. Insets presents the micrograph of the *C. closterium* cell under 20x (left) and 100x magnification (right).

3.2. Non-resonance excitation of solid-state fucoxanthin and β -carotene: differentiation of carotenoids in complex biosystems

The experimental $\nu_1(\text{C}=\text{C})$ envelope of solid state β -carotene was centred at 1513.1 cm^{-1} , with a FWHM of 16.85 cm^{-1} . The band assignments were previously discussed by Cintă Pinzaru et al. (2015). The analysis of the experimental ν_1 band shape with Lorentzian multi-peaks fit showed two components (Figure 8a), at 1512.2 and 1520.5 cm^{-1} with the area ratio of 7.603 ($R^2 = 0.998$). DFT calculations were done for the isolated, fully relaxed β -carotene molecule. Applying the Lorentzian multi-peaks fit to the calculated band shape, resulted in the best fit ($R^2 = 0.999$) for two components at 1517 and 1525 cm^{-1} , likewise spaced about 8 cm^{-1} (Figure 8b).

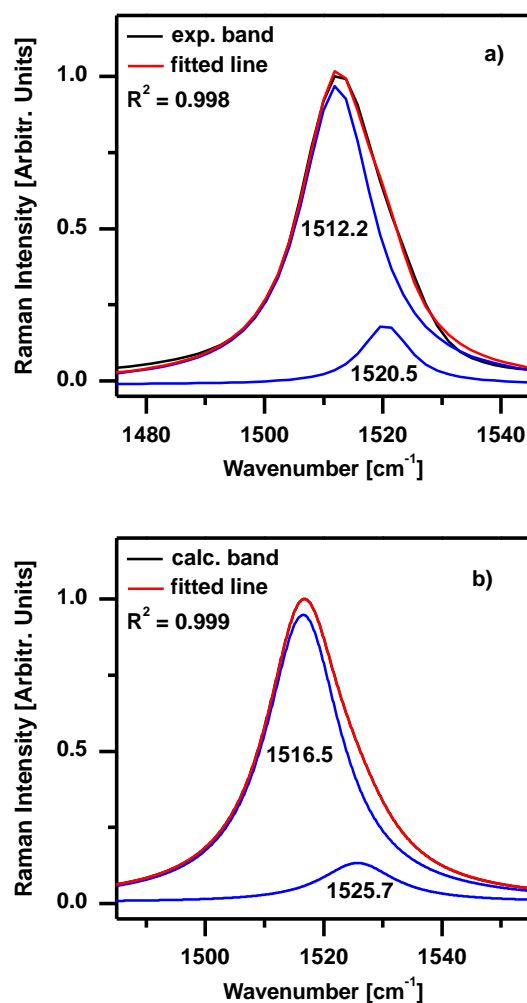


Figure 8. Deconvolution of (a) experimental and (b) theoretical b-carotene ν_1 band into two Lorentzian components. Spectra are normalized to $\nu_1(\text{C}=\text{C})$ intensity.

Theoretical calculations were done for 3 conformers of the fucoxanthin molecule in vacuum, c1, c2, and c3, with predicted Boltzmann populations of 62, 35 and 3 %, respectively. Experimental spectra show that the 532 nm laser line, although not near the absorption maximum, still promotes electronic transitions in solid fucoxanthin as observed by prominent overtones in 2400-3200 cm^{-1} range, while the 632.8 and 785 nm lines do not. Although the c1 is predicted to be the most abundant conformer in vacuum, the experimental spectrum of solid features most similarities with c3, in terms of $\nu_1(\text{C}=\text{C})$ width and the shape of ν_2 and ν_3 regions.

The Lorentzian multi-peaks fit of the ν_1 band acquired *in situ* from *C. closterium* revealed four components (Figure 9). The one at 1531 cm^{-1} is assigned to FX_{red} within the FCP, in line with Premvardhan et al. (2009). The most intense component at 1525 cm^{-1} likely also reflects fucoxanthin contribution, but it does not fit the usual FCP frequency range. It does, however, approach the position of fucoxanthin organic crystals excited with the same laser, hence it is tentatively assigned here to a possible population of fucoxanthin which is not bound in FCP.

These two components represent 62% of the total ν_1 area. Cintă Pinzaru et al. (2016a) previously recorded RR ν_1 (C=C) band from *C. closterium* at 1528 cm^{-1} ; however, that study considered it as a single mode.

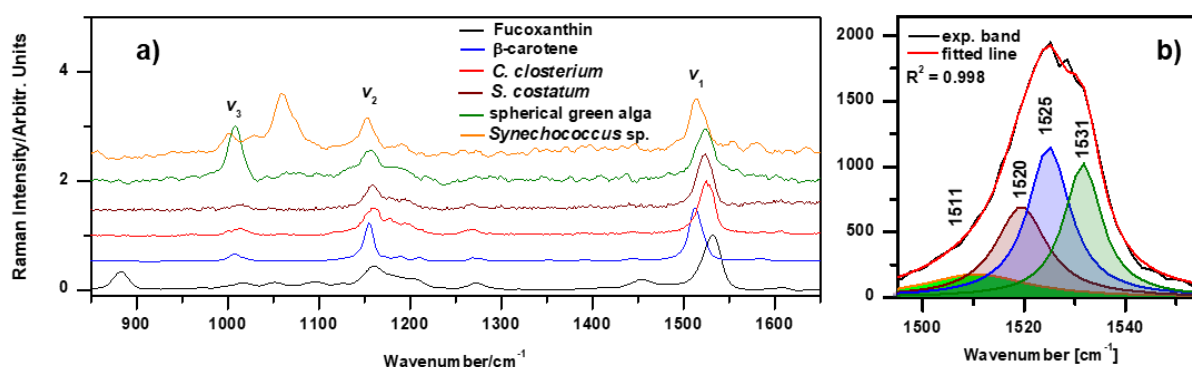


Figure 9. a) Micro-Raman spectra of single cells of photosynthetic microorganisms and the reference carotenoids, as indicated; b) Lorentzian multi-peaks fit of the ν_1 band envelope from the *C. closterium* diatom from (a), showing the contributions of individual carotenoid pools.

3.3. Effect of metallic nanoparticles aggression on the carotenoid Raman signal of cyanobacteria on cellular level

The typical Raman spectrum of native *C. pussilum* cells, recorded under 532 nm excitation, features the three strongest carotenoid bands at 1515, 1154 and 1002 cm^{-1} , on top of a high fluorescence background presumably arising from the abundant chlorophyll (Figure 10). Analysis of a larger number of cells was attempted, however, in most cases the fluorescence level exceeded the count limit and oversaturated the CCD detector, hence only 5 to 6 successful micro-Raman spectra were saved from different cells, from each group (control and treated) at each analysis point. Subtraction of the background results in a low-quality carotenoid signal with a high amplitude of noise. This kind of signal is consistent with previous reports of micro-Raman analysis of single cyanobacteria cells, containing relatively low amount of scattering material (Cintă Pinzaru et al., 2016b). Nevertheless, these results represent the first *in situ* detection of carotenoids in the cyanobacteria *C. pussilum* AICB 1012 strain.

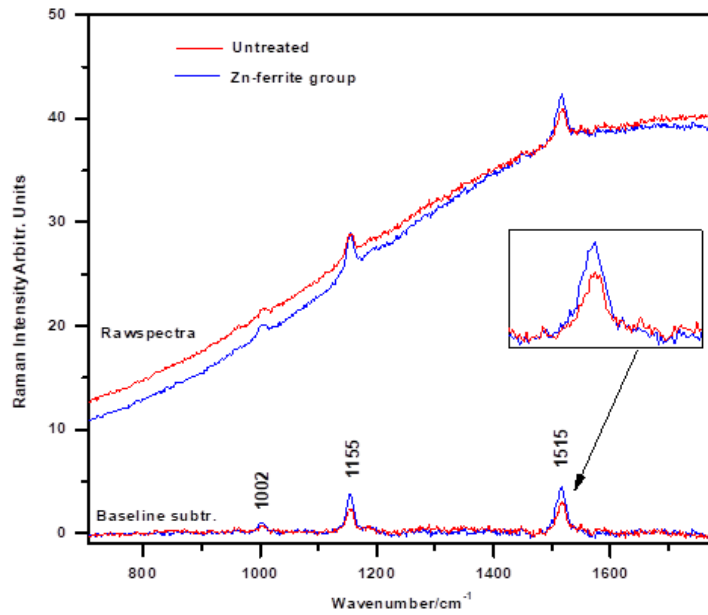


Figure 10. Aspects of processing of the Raman spectra from single cyanobacteria cells (*Coelomorion pussilum* AICB 1012), shown here using the example of control group and that treated for 24 hours with Zn-ferrite nanoparticles.

Five to six spectra from each measurement stage were averaged, and the relative intensity of carotenoid ν_1 band to the background intensity at 1515 cm^{-1} (under the band centre) was expressed as a ratio, $R = I_{\text{carotenoid}}(1515) / I_{\text{background}}(1515)$ (Figure 11). The chlorophyll fluorescence (background) is not measured directly in Raman spectroscopy; however, the background can still hold valuable information about the sample.

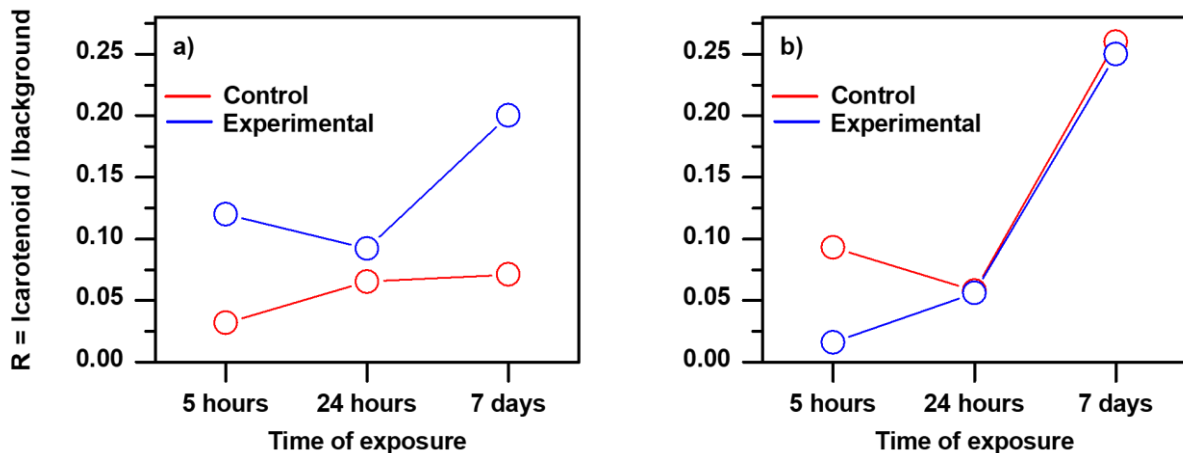


Figure 11. Plot of the evolution of R [$R = I_{\text{carotenoid}}(1515) / I_{\text{background}}(1515)$] through the sampling points at 5 and 24 hours, and 7 days of exposure, for the Zn-ferrite (a) and the Mn-Zn ferrite (b) nanoparticles treatment.

3.4. Manganese zinc ferrite nanoparticles and their Raman spectroscopy - original research article

- *Published in Journal of Raman Spectroscopy, on 12. February 2020, Impact factor (2018) = 2.80*
 - Citation: Nekvapil, F., Bunge, A., Radu, T., Cinta Pinzaru, S, Turcu, R. Raman spectra tell us so much more: Raman features and saturation magnetization for efficient analysis of manganese zinc ferrite nanoparticles. *J. Raman Spectrosc.* 2020b, 51(6): 959-968. DOI: 10.1002/jrs.5852
- *Oral presentation at the 12th International conference "Processes in Isotopes and Molecules, Cluj-Napoca (Romania), 25th -27th September 2019*
 - Citation: Nekvapil, F., Bunge, A., Radu, T., Cinta Pinzaru, S., Turcu, R. Raman spectroscopy analysis of metal-ferrite nanoparticles: towards precise interpretation and extraction of structural information. In: *Book of Abstracts of the 12th International Conference Processes in Isotopes and Molecules.* National Institute for Research and Development of Isotopic and Molecular Technologies, Cluj-Napoca, 25th - 27th September 2019, p. 17.

In this study, we aimed to obtain solid and detailed knowledge on Raman spectroscopy output of the nanoparticles of the type that would be used in the toxicological study on cyanobacteria described in the Section 3.3. As outlined in the introductory lines of the Section 3.3. and of the following publication, many kinds of nanoparticles with different composition, structure and properties are manufactured to accomplish various purposes, which may finally reach the water bodies and other environments. Following this study, the manganese-zinc ferrite ($\text{Mn}_{0.8}\text{Zn}_{0.2}\text{Fe}_3\text{O}_4$) nanoparticles can be identified by Raman spectroscopy, and their magnetic properties, i.e. amount of lattice defects (via the 713 cm^{-1} band) estimated. Hence, the nanoparticle type and magnetic properties can be properly linked to the carotenoid Raman signal resulting from the cell interaction (Section 3.3.3.). Such a correlation contribute to the broader Thesis aim of extension of Raman applications to the environmental fields.

3.5. Chapter 3. conclusions

The specificity of fucoxanthin Raman and SERS signal, and the complex $\nu_1(\text{C}=\text{C})$ band shape was addressed by high precision experimental Raman techniques and theoretical calculations, and the prospects for detailed spectral interpretation, identification and quantification of this carotenoid were presented.

Under normal Raman excitation, the fucoxanthin signal intensity, expressed as the intensity of the $\nu_1(\text{C}=\text{C})$ band relative to the intensity of ethanol $\nu(\text{C}-\text{H})$ band, increases linearly in the concentration range 1.201 - 60.042 $\mu\text{mol l}^{-1}$, while the SERS signal, expressed as the $\nu_1(\text{C}=\text{C})$ band intensity relative to the water $\nu(\text{O}-\text{H})$ band follows a third order polynomial trend in the range 0.024 - 12.008 $\mu\text{mol l}^{-1}$.

The claims stating the ambiguity of the capability of Raman spectroscopy to determine the carotenoid profile of biological systems, found in a part of the literature, arise from superficial interpretation of spectra, namely taking into consideration only the frequency of ν_1 , ν_2 and ν_3 envelopes (Jehlička 2014; de Oliveira et al., 2010). This Thesis shows that careful consideration of Lorentzian multi-peaks deconvolution (or even fitting with a single profile, when relevant) of the ν_1 band shape, taking into account the frequency-FWHM-laser line relationship effect, allows the carotenoids differentiation and identification.

Single-cell micro-Raman spectroscopy can be used to probe slight changes in carotenoid content of the cyanobacteria treated with ferrite nanoparticle. relative to untreated culture. The physiological response of the cyanobacteria is observed in terms of the ν_1 band position and the intensity ratio of the ν_1 band and the fluorescence background level below the band. The colloidal character of AgNPs causes the greater extent of coverage of cells, while the magnetic character of ferrite NPs causes them to clump with each other, rather than adhering to the cells, as evidenced by electron microscopy.

Combination of micro-Raman and electron microscopy, which required almost no sample preparation in the presented case, show potential for rapid ecotoxicological testing of physiological effect of NPs on cyanobacteria and the visualization of their interaction. However, the method shows huge potential for further improvements.

4. COMPARATIVE TISSUE ANALYSIS, *IN SITU* DETECTION AND BIOCHEMICAL ROLES OF CAROTENOIDS STUDIED BY RESONANCE RAMAN AND SERS; DELICATE TISSUE PREPARATION AND PRESERVATION FOR RAMAN ANALYSIS

Raman spectroscopy techniques broadly recognized as holding the potential for high-sensitivity and high-precision analysis in the fields of marine biology, biotechnology and biophysics, with the large number of studies focusing on microorganisms. However, exemplary in-depth studies applying Raman spectroscopy for analysis of carotenoids within native tissues and tissue extracts of multicellular marine organisms, that actually demonstrate this analytical potential with real-world relevance, are scant in the existing literature. Also, little is known about the proper and effective sample preparation for Raman analysis *in vivo*, or as close to the native system state as possible.

In this Chapter, we employed comparatively Resonance Raman spectroscopy and SERS to demonstrate the detection, identification and metabolism of carotenoids and study their role in cellular protection and stress response in different tissues of sea urchins as model invertebrates. Apart from more than a century of research tradition as a biological and toxicological models (di Bernanrdo and di Carlo, 2017), their gonads present a luxurious food product with a significant market turnover in coastal areas and famous seafood markets, owing to their high carotenoid content (McBride et al., 2004).

The carotenoids were comparatively analysed 1) across the tissues within the same species, 2) between corresponding tissues of two sea urchin species, and 3) between sea urchin body fluid and the surrounding sea water. We conducted Raman analysis on native tissue where possible. In cases where carotenoids had to be extracted, we employed as simple and minimal sample treatment as possible, in order to prospect carotenoid analysis with cost- and labour-efficiency in mind. Furthermore, we infer the stress response roles of carotenoid based on their Raman signal under resonance excitation and SERS conditions, and the features of particular carotenoids known from the literature.

4.1. Comparative study of carotenoid metabolism in sea urchins studied by Resonance Raman spectroscopy and SERS techniques

Accepted as and oral presentation to the International Conference of Raman Spectroscopy, Rome, 1.-6. August 2021

4.1.1. Carotenoids detection and characterization in echinoderms

This section presents a collection of comparative studies of tissue carotenoid content of the two sea urchin species, the stony sea urchin *Paracentrotus lividus* and the black sea urchin *Arbacia lixula*, with the aim of prospecting the similarities and differences in their Raman output, and consequently tissue carotenoid content. The initial hypothesis holds that their tissues will contain different carotenoids, reflecting the different carotenoid profiles of the sources the two species feed on. Raman spectroscopy and its techniques (Resonance Raman, SERS) show a great promise for probing this hypothesis. In addition to the main finding, several other conclusions on practical aspects of sample preparation and analytical approach are drawn.

4.1.2. General sampling procedures

Sea urchins were collected from shallow a shallow pier in the Bay of Gruž, Dubrovnik city on several occasions in the period 2017 - 2019. It was observed that,

P. lividus is usually found on bottom rocks, while *A. lixula* was attached to vertical concrete surfaces. The sea urchins were collected using a hand-held net and transported to the University of Dubrovnik in the proximity of the collection site for initial sample preparation. Each tissue required different preservation/extraction procedures, which were established through several years of collaboration of the Raman-AFM Laboratory (Babeş-Bolyai University) and the Department of Aquaculture (University of Dubrovnik), and will be discussed in the following respective sections.

4.1.3. SERS detection of carotenoids in the digestive system extracts

A Lorentzian multi-peaks fit of the $\nu_1(\text{C}=\text{C})$ band from the spectrum 2 which features the clearest band, is shown in the Figure 4.1.1.d (full-length Thesis). The fit revealed one strong component at 1532 cm^{-1} , assigned here to fucoxanthin/fucoxanthinol (reference spectrum included in Figure 4.1.1.c), and another strong component at 1523 cm^{-1} , which is tentatively assigned here to canthaxanthin, lutein or α -carotene (Bernstein et al., 2002), which are known to occur in certain species of green and brown algae (Abd El Baky et al. 2008; Casazza and Mazzella, 2002). The last, and weakest component at 1513 cm^{-1} fits well the ν_1 feature of solid state β -carotene (Cintă Pinzaru et al., 2015; Section 3.2.).

4.1.4. SERS detection of carotenoids in the coelomic fluid

The four main carotenoid bands, at 956 , 1010 , 1157 and 1525 cm^{-1} , have been recorded from the *P. lividus* coelomic fluid ethanolic extract, although with wide variation of intensity. On the other hand, the samples of *A. lixula* featured multiple signals of organic material, but no clear carotenoid signals; Rygula et al. (2013) and Czamara et al. (2014) have presented detailed reviews of protein and lipid Raman bands, respectively. The $1400 - 1600\text{ cm}^{-1}$ range in *P. lividus* spectra was too complex for precise baseline subtraction and fitting with Lorentzian shapes. Nonetheless, certain differences were observed: the main in-plane C=C band shifted from 1527 cm^{-1} in the digestive system to 1525 cm^{-1} in the coelomic fluid, and the out-of-plane C=C bands appeared at 1580 and 1602 cm^{-1} , indicating additional metabolic processes taking place presumably in the gut wall.

4.1.5. Echinenone and β -carotene of sea urchin gonads - effect of molecular environment on the carotenoid Raman bands

The SERS spectra acquired from gonad ethanolic extracts from 7 *P. lividus* females featured the well-recognizable signal of carotenoids, including the ν_1 at 1520

cm^{-1} , ν_2 at 1154 cm^{-1} , the ν_3 at 1004 cm^{-1} , and the bands at 1366 , 1585 and 1615 cm^{-1} which are enhanced as a result of interaction of carotenoids with the AgNPs (Cintă Pinzaru et al., 2015). When analysing several dozens of SERS spectra, a variation of ν_1 frequency between 1518 and 1522 cm^{-1} can be observed. This variation was attributed by Nekvapil et al. (2019) to the variation in relative contents of β -carotene (1512 cm^{-1}) and echinenone (1521 cm^{-1}) throughout the reproductive cycle of the sea urchins. This issue is discussed in more detail in section 4.3.

4.1.6. Resonance micro-Raman detection of carotenoids in native sea urchin eggs

Native, untreated *P. lividus* and *A. lixula* dry eggs deposited on a reflective SpectRIM plate are convenient for conventional micro-Raman analysis, exhibiting strong signal of carotenoids both under resonant and non-resonant excitation (Nekvapil et al., 2019). Prominent carotenoid signal, consisting of contributions of echinenone and β -carotene could be recorded from any point within the eggs, and their distribution appears to be uniform throughout the entire cells (Nekvapil et al., 2019). On the other hand, *A. lixula* eggs contained several regions of different spectral pattern: 1) the signal from darker regions at the cell perimeter featured only the signals of lipids and proteins, 2) yellowish regions within eggs featured a weak carotenoid signal, and 3) the well-recognizable carotenoid main bands could be recorded from the reddish “pockets” of presumably higher carotenoid content.

4.1.7. Resonance micro-Raman localization of the carotenoid signal in larvae

Carotenoid signal could have been recorded at skeletal rods in both species, while in *P. lividus* larvae carotenoid signal was also recorded from vivid red pigment granules (Figure 12c). In both species, the ν_3 and the ν_2 bands were recorded at 1004 and 1154 cm^{-1} , respectively, while the ν_1 was recorded at 1514 cm^{-1} in *P. lividus* and at 1517 cm^{-1} in *A. lixula*. The band envelope shape analysis by Lorentzian multi-peaks fitting shows that ν_1 contains in both species strong contribution of β -carotene (1512 cm^{-1}) and echinenone (1521 cm^{-1}). However, in *P. lividus*, the β -carotene mode is notably stronger ($\text{area}_{\beta\text{-carotene}} / \text{area}_{\text{echinenone}} = 4.29$), while in *A. lixula* the two modes were of similar intensity ($\text{area}_{\beta\text{-carotene}} / \text{area}_{\text{echinenone}} = 1.33$), hence the shift of band envelope maximum.

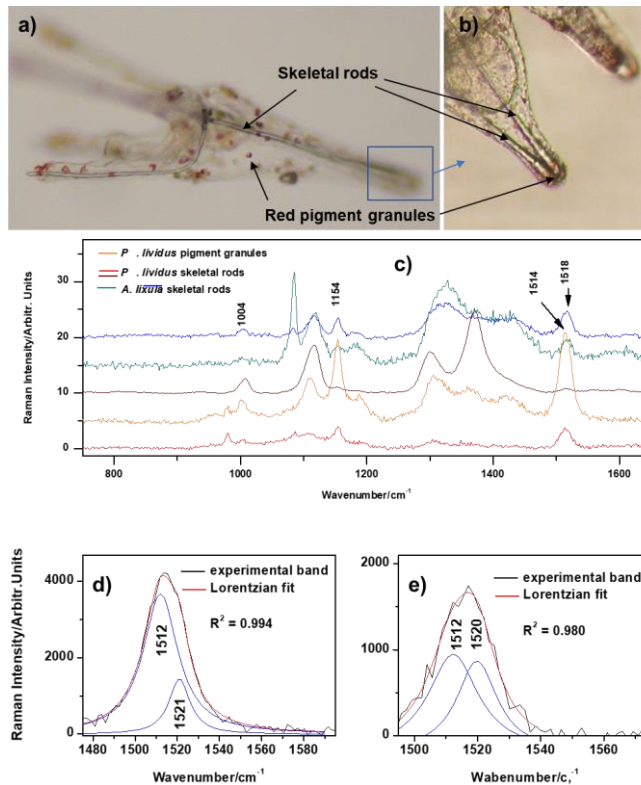


Figure 12. Micrograph of a sea urchin *Paracentrotus lividus* larva in the 4-arm pluteus stage, with skeletal rods and pigment granules indicated; (b) enhanced view of the growing tips of the skeletal rods at the posterior side of another larva; (c) comparative display of micro-Raman spectra acquired from the pigment granules and skeletal rods of the larvae of the sea urchins *P. lividus* and *Arbacia lixula*. Lorentzian multi-peaks fits of the $\nu_1(\text{C}=\text{C})$ region are also presented for a spectrum acquired from *P. lividus* (b) and *A. lixula* (c) skeletal rod.

4.2. Comparative Raman spectroscopy study of the coelomic fluid of grazing sea urchins and their native seawater: prospect for a potential indicator of environmental aggression

- *Published as in-extenso proceeding to the international conference “Air and Water Components of the Environment”, Sovata, coupled with the oral presentation*
 - Citation: Nekvapil, F., Tomšić, S., Cintă Pinzaru, S. Comparative Raman spectroscopy study of the coelomic fluid of grazing sea urchins and their native seawater: prospect for a potential indicator of environmental aggression. In: Şerban, G., Băţinaş, R., Tudose, T., Horváth, Cs., Croitoru, A., Holobăcă, J. (eds.) Air and water Components of the Environment, University Press, Cluj-Napoca, ISSN: 2067-743; 2018b, p. 27 – 34.

Abstract

Sea urchins have limited ability to move, and they use the watervascular circulation system to pump surrounding sea water in order to set body parts in motion. It is therefore thought that coelomic fluid, a body fluid of sea urchins which acts as its internal transport and immune system, contains metabolised pollutants. In the present study, we developed a method for detection of carotenoids in the coelomic fluid by Raman spectroscopy. Carotenoids were obtained from the coelomic fluid by ethanol extraction and their selective resonance Raman signal was enhanced employing the surface enhanced Raman scattering (SERS) technique. Carotenoids are ingested by sea urchins through their plant-based diet, metabolised and transported into the coelomic fluid, where they were detected for the first time via SERS. We further investigated the correlations of carotenoids signalling from the coelomic fluid with the local sea water to prospect a potential linkage with changes under environmental aggression. The antioxidative and immunomodulatory role of carotenoids, especially of β -carotene, was extensively studied in vertebrates (Chew and Park, 2004). Biological defence and increased antioxidant activity is associated with an increased carotenoids level and/or change in their species balance in native sea urchins. Additionally, we compared relative sulfate concentration of sea urchin coelomic fluid with local sea water using FT-Raman technique. We discuss the possibility for development of methods for rapid and cost effective monitoring of the native environmental waters via sea urchin carotenoids. Other co-existent pollutants which may enter the coelomic fluid via the digestive system or through water-vascular system of sea urchins are expected to correlate with the animal response via an increased antioxidant activity due to carotenoids. Thus, sea urchins may prove to be good sentinels of environmental water changes via their carotenoids signalling.

Keywords: environmental water, pollutants, sea urchins, Raman spectroscopy.

4.3. Microsphere packages of carotenoids: intact sea urchin eggs tracked by Raman spectroscopy tools - original research article

- *Published in Photochemical & Photobiological Sciences, on 23. May 2019, Impact factor = 2.40*
 - Citation: Nekvapil, F., Brezeştean, I., Tomšić, S., Müller, Cs., Chiş, V., Cintă Pinzaru, S. Microsphere packages of carotenoids: intact sea urchin eggs tracked by Raman spectroscopy tools. Photochem. Photobiol. Sci. 2019a, 18: 1933-1944. DOI: 10.1039/c9pp00181f.
- *Oral presentation at the 18th International conference Prospects for 3rd Millennium Agriculture, ClSuj-Napoca (Romania), 27th - 29th September 2018*

- Citation: Nekvapil, F., Brezeştean, I., Tomsic, S., Muller, Cs., Chis, V., Cintă Pinzaru, S. Rapid and cost effective tracking carotenoids in native sea urchin eggs by multi-laser Raman spectroscopy. In: Vodnar, D.C. (ed.) Book of Abstracts. Faculty of Agricultural Sciences and Veterinary Medicine of Cluj-Napoca, 2018.

Carotenoids are an important determinant of market value of the gonads, contributing to their colour and organoleptic properties (McBride et al., 2004). In the following paper we have employed Resonance Raman (532 nm) *in situ* analysis of the native eggs and the gonad extracts, and NIR-Raman (785 nm) on the eggs only, to study the carotenoids profile and the overall chemical composition of the eggs. Here we have shown that RRS signal of the native eggs can reveal the content of the carotenoids echinenone, β -carotene and other minor species after a simple Lorentzian multi-peaks deconvolution, thus providing a rapid method for the egg carotenoids assessment. Since eggs fill the mature, pre-spawning gonads, *in situ* analysis of the native eggs by RRS is a simpler and more rapid method than the extraction of the bulk gonad tissue and subsequent analysis of the extracts, and further development of portable Raman spectrometers will allow the true on-site implementation of gonads quality control at the site of retail. This will allow the expansion of the applicability of Raman spectroscopy tools in both the biology research and on the seafood market, thereby supporting the Thesis aims.

4.4. Exploring the biological protective role of carotenoids by Raman spectroscopy: mechanical stress of cells - original research article

- *Published in Studia Universitatis Babeş-Bolyai Physica, on 30. December 2019*
 - Citation: Nekvapil, F., Molnar Muller, Cs., Tomsic, S., Cintă Pinzaru, S. Exploring the biological protective role of carotenoids by Raman spectroscopy: mechanical stress of cells. Studia UBB Physica 2019b, 64: 75-82. DOI: 10.24193/subbphys.2019.08

There are ample suggestions that carotenoids contribute to the cellular chemical defence by their free radical scavenging activity (discussed in the Section 4.3.). However, the following paper aimed to elucidate if the carotenoids play a role also in the mediation of a physical stress in sea urchin eggs, i.e. if any difference in the carotenoid Resonance Raman (and SERS) signal can be observed between mildly centrifuged sea urchin eggs and the untreated ones. The clear increase of the carotenoid SERS signal was localized near the egg periphery under the SERS approach, indicating that the carotenoids were indeed mobilized in response to this physical stress. Hence, the knowledge of carotenoids behaviour under the physical

stress and inherent protection of cells is expanded, in line with the aim of the Chapter 4 regarding further investigation of the biological functions of carotenoids.

4.5. Chapter 4 conclusion

Further conclusions on the detection and the behaviour of carotenoids Raman signal related to the marine biochemistry research are achieved:

- Surface-enhanced Raman scattering allowed the detection of carotenoid signal in tissue extracts where only the signal of the solvent or the fluorescence could have been recorded under spontaneous Raman scattering.
- Resonance Raman (micro)spectroscopy technique allowed the *in situ* detection of the carotenoid signal in the dry gonad extract, the eggs and the larval tissues. Under non-resonant excitation, these tissues exhibit relatively stronger signals of non-target compounds (proteins and lipids), as shown by Nekvapil et al. (2019).
- Lorentzian multi-peaks deconvolution of the $\nu_1(\text{C}=\text{C})$ carotenoid band with relevant number of (2 - 4) components with meaningful positions and widths allows the differentiation of contributions of individual carotenoid pools (fucoxanthin derivatives, echinenone, β -carotene, astaxanthin etc.). The fitting procedure yields more precise results than the considerations of only the global band envelope properties.
- Raman spectroscopy tools, the Resonance Raman and SERS, are shown here to be suitable for probing of the biochemical functions of carotenoids in invertebrate tissues: Section 4.2. suggests that the carotenoid profile of the sea urchin coelomic fluid, obtained by SERS measurements, may change in response to the environmental aggression, similar to the presumed increase of β -carotene signal in cyanobacteria exposed to the ferrite nanoparticles (Section 3.4.); Resonance Raman detection of accumulation of greater amounts of echinenone and β -carotene in the native eggs (Section 4.3.) indicated their role as the cellular antioxidant reserve; localization of carotenoids to the egg cell periphery, determined by the combination of SERS and RRS, indicates that the carotenoids are also mobilized in response to the physical stress.

5. CHANGE OF OPTICAL PROPERTIES OF CAROTENOIDS UPON BINDING TO PROTEINS CRUSTACYANINS INVESTIGATED BY RESONANCE RAMAN WITH MULTIPLE LASER LINES AND BY DFT; SIMILARITIES OF THEIR SIGNAL TO UNSATURATED POLYENES; APPLICATION OF RAMAN SPECTROSCOPY IN BLUE BIOECONOMY AND CIRCULAR ECONOMY

Upon binding into the crustacyanin complex, the carotenoid astaxanthin undergoes a prominent bathochromic shift in its absorption spectrum and Raman signal, shifting the absorption maximum from 460 - 470 to 580 - 630 nm range, and from 1514 to 1490 - 1498 cm^{-1} range, respectively. Both pigment types (free astaxanthin and astaxanthin-crustacyanin complex) were previously proven by Resonance Raman spectroscopy *in vivo* only in lobster shell (Salares et al., 1977), hence it is commonly believed that the pigment α -crustacyanin is specific to the blue or purple crustacean shells.

The mechanism of this shift in the spectroscopy output was studied on multiple occasions by computational techniques, with the each study explaining only a part of the reason of the shift, but not the entire account. These viewpoints raised some controversies, and the mechanism of the bathochromic shift is still not fully explained

To contribute to the unravelling of this discussion, we conducted a series of *in situ* Resonance Raman studies (532 nm for astaxanthin, 632 nm for crustacyanin, 785 nm non-resonant) to detect the two types of pigments in crustacean shells of various colours. The detection of both pigments in shells of almost all species indicated at first glance that crustacyanin is not specific for blue-coloured shells, as previously believed (Sections 5.1., 5.2. and 5.3.).

We also conducted DFT calculations on isolated astaxanthin (simulating the carotenoid in its free form) and on astaxanthin in the presence of a water molecule (simulating non-covalent bonding to the crustacyanin), computing the Raman shift of astaxanthin $\nu_1(\text{C}=\text{C})$ component from 1508 cm^{-1} (free form) to 1494 cm^{-1} (non-covalently bonded form) (Section 5.3.).

Additionally, scanning electron microscopy revealed the colour-specific shell porosity on nano scale, which sparked our interest to investigate the structural colour of the crab shells (Section 5.2. and 5.3.), and to promote the crustacean shells comprising a part of inedible food waste into novel porous biomaterials with interesting mineral composition and wide potential applicability in agriculture, industry and biomedicine (Sections 5.4. and 5.5.).

5.1. Resonance Raman signal of crustacean pigments located in a porous biogenic carbonate structures - controversies and new breakthroughs on the origin of colour

Recently, Nekvapil et al. (2020) reported that the Raman-active pigment profile of the two crab species, the Atlantic blue crab (*Callinectes sapidus*) and the Mediterranean green crab (*Carcinus aestuarii*) is qualitatively the same, and dominated by the orange astaxanthin and blue crustacyanins. The colour difference is explained by different ratio of the chromophore abundance and shell nanopores of different diameter acting as a natural supergrating in red, blue, white and green shell parts. Here we have employed the micro-Raman spectroscopy approach using resonance excitation for free carotenoids (532 nm) and crustacyanin-type carotenoproteins (632.8 nm) which enables to study each pigment group separately, and evidence their diversity in native cuticles of 13 species of crustaceans from different taxa, comprising a total of 16 cuticle anatomical parts. Additionally, the non-resonant 785 nm line provided simultaneous recording of both pigments with low level of fluorescence background. We show that the crustacean Raman-active pigments (carotenoids) are different than the unsaturated polyenes previously detected in shells of other invertebrates (Wade et al., 2019; Hedegaard et al., 2006; de Oliveira et al., 2013), and we discuss the spectroscopic differentiation between the four presumptive groups of polyene-based pigments of invertebrate shells.

Figure 13. summarizes our findings on the carotenoid and carotenoprotein signals following the micro-Raman analysis of native shells of 8 crustacean species (10 anatomical parts). Raman spectra from all crustacean shells excited under all three laser lines (532, 632.8 and 785 nm) featured the three main carotenoid bands: the ν_1 between 1490 and 1520 cm^{-1} , the ν_2 around 1154-1157 cm^{-1} and the ν_3 around 1004 cm^{-1} . The presence of the ν_3 band and the position of the ν_2 above 1155 cm^{-1} confirms the presence of $-\text{CH}_3$ groups attached to the polyene chain, characteristic to carotenoids. Unsaturated polyenes, where the polyene chain is not fully methylated, would on the other hand, not exhibit the ν_3 band, and the ν_2 would usually appear between 1120 and 1145 cm^{-1} (Hedegaard et al., 2006; de Oliveira et al., 2013; Wade et al., 2019). Different excitation lines revealed that the great variation of the position and width of the ν_1 band is in fact due to its two-component character: the contribution of free carotenoids is enhanced by the 532 nm line (1510 - 1530 cm^{-1} ; Salares et al., 1979; this Thesis) and the contribution of carotenoproteins is enhanced by the 632.8 nm line (Salares et al., 1979; Chapter 5).

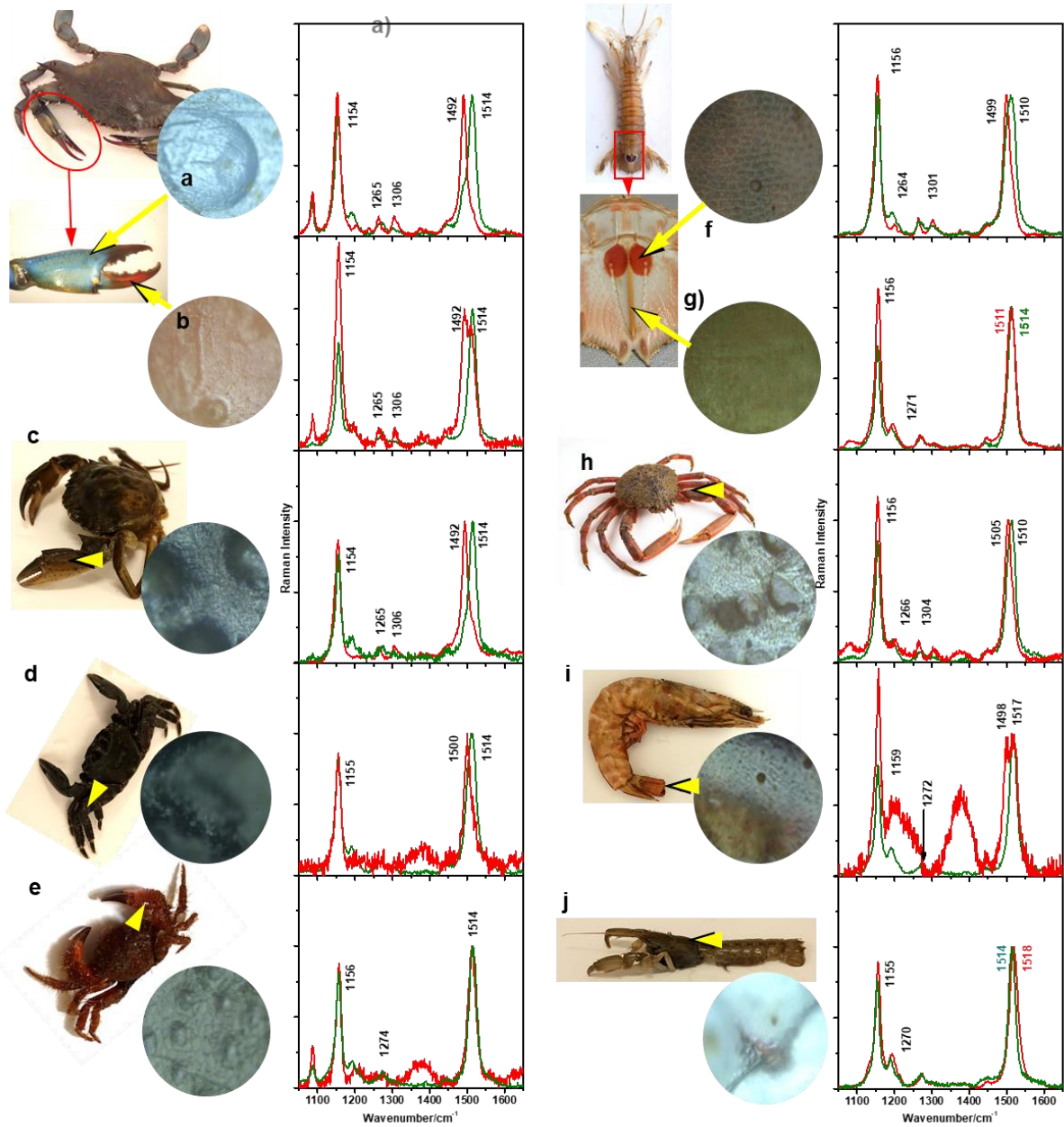


Figure 13. Micro-Raman spectra acquired under 532 (green lines) and 632.8 nm (red lines) excitation, from surface of 10 crustacean shells types of different colours, as shown in photographs: (a) and (b) *Callinectes sapidus* blue and red claw shell, respectively; (c) *Carcinus aestuarii*; (d) *Pachygrapsus marmoratus*; (e) *Pilumnus* sp.; (f) and (g) *Squilla mantis* red “eyespot” and telson medial carina, respectively; (h) *Maja squinado*; (i) *Melicertus kerathurus*; (j) *Upogebia pusilla* (transparent cuticle). Spectra are normalized to unity for easier comparison. Yellow arrows indicate points of spectra acquisition from the crab shells, and micrographs (round insets) show the shell surface color and morphology of the probed area under 200x magnification.

5.2. Natural nanoarchitecture of Blue crab (*Callinectes sapidus* Rathbun, 1896) claw studied by Raman spectroscopy and scanning electron microscopy

Oral presentation at the International Balkan Workshop on Applied Physics, Constanța 2017

Citation: .Nekvapil, F., Tomšić, S., Glamuzina, B., Barbu-Tudoran, L., Brezestean, I., Cintă Pinzaru, S., Natural nanoarchitecture of blue crab (*Callinectes sapidus* Rathbun, 1896) claw studied by Raman spectroscopy and Scanning electron microscopy. In: Vladoiu, R., Mandes, A., Dinca Balan, V. (eds.) Conference proceedings. Issue 17/2017, University of Ovidius Press, p. 146 – 147.

This Section shows our first results on deeper investigation of the colour of the Blue crab, *C. sapidus*, following the inherent scientific interest into the complex origin of invertebrate shell colour components outlined in the Section 5.1. Four laser lines were employed to non-destructively characterize the Raman scattering signal of the complex exoskeleton of the blue crab (*Callinectes sapidus*) claw (Figure 14). Four distinct compounds could be identified and localized within the complex nanoarchitecture. The astaxanthin (AXT), biogenic magnesian calcite and astaxanthin-crustacyanin complex (ACC) were unambiguously differentiated for the first time in the complex exoskeleton. Chitin trace was detectable using the near infrared line. Complementary information from SEM EDX analysis combined with micro Raman data and images allowed to provide for the first time a complete structural characterization and to critically address a recent study (Katsikini, 2016) of the blue crab shell employing 488 nm laser, claiming the carotenoid chromophore only responsible for the various colours, and the presence of Sr and Br in the calcite skeleton. The 532 nm laser line, which is near-resonant for AXT, is not resonant for the ACC, but the 632 nm line falls within the full resonance of the latter. The 830 nm laser line showed prominent Raman peaks of magnesian calcite and not calcite and vaterite as previously claimed¹, and trace of chitin (Fig. 5.2.1.). The target area was also examined using scanning electron microscope to study the natural nanoarchitecture (Fig. 1). This study highlights the importance of informed choice of laser line for drawing correct conclusions on the complex natural biocomposites.

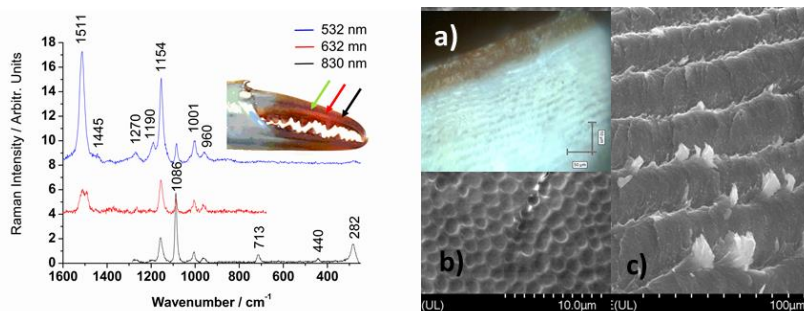


Figure 14. Representative Raman spectra of the outer red surface of the blue crab claw, excited with 532, 632 or 830 nm laser line as indicated, revealing the astaxanthin, alpha- ACC and magnesian calcite, respectively with trace chitin ; (a) Cross section, microscopy view, b) and c) SEM images from the outermost, red surface and the nanoarchitecture of the layers.

5.3. Color-specific porosity in double pigmented natural 3d-nanoarchitectures of blue crab shell - original scientific article

-

- *Published in Scientific Reports, on 20 February 2020, Impact factor 4.01*
 - Citation: Nekvapil, F., Cintă Pinzaru, S., Barbu-Tudoran, L., Suciu, M., Tamas, T., Chis, V. Color-specific porosity in double pigmented natural 3d-nanoarchitectures of blue crab shell. *Sci. Rep.* 2020b, 10: 3019. DOI: 10.1038/s41598-020-60031-4.

In this study, we address the long-standing discussion and the issue of controversies regarding the underlying mechanisms of the bathochromic shift of the absorption band of astaxanthin, and related red-shift of the $\nu_1(\text{C}=\text{C})$ Raman band upon binding to the crustacyanin. We demonstrate that the Raman ν_1 band is indeed shifted upon non-covalent binding (ncb) to the crustacyanin, as shown by comparison of the Raman activity of isolated astaxanthin, and astaxanthin in the presence of a water molecule. Further Resonance Raman investigation using multiple laser lines allowed the in-situ detection of signals of both free and ncb-astaxanthin. Additionally, high-resolution SEM allowed evidencing of the structural component of the complex colour origin puzzle, by revealing the natural shell nanoarchitecture composed of regularly arranged nanometric channels. The paper presents valuable new knowledge on the behaviour of carotenoproteins in natural matrices.

]

5.4. From Blue bioeconomy toward Circular economy through high-sensitivity analytical research on waste Blue crab shells - original research article

- *Published in ACS Sustainable Chemistry and Engineering, on 11. September 2019, Impact factor (2020) = 7.03*
 - Citation: Nekvapil, F., Aluas, M., Barbu-Tudoran, L., Suci, M., Bortnic, R-A, Glamuzina, B., Cintă Pinzaru, S. From Blue Bioeconomy toward Circular Economy through High-Sensitivity Analytical Research on Waste Blue Crab Shells. Sustainable Chem. Eng. 2019c, 7: 16820-16827. DOI: 10.1021/acssuschemeng.9b04362. Copyright © 2019, American Chemical Society

In this paper, we employed the insights on the analytical possibilities of the Resonance Raman spectroscopy and electron microscopy applied to the crustacean shells. The following paper presents a sustainability-driven research into the possibility of the re-use of abundant crab shell which are currently being disposed as waste. The carotenoid and carotenoprotein RRS signal is used here as a sensitive molecular marker, which indirectly indicates that useful, delicate compounds from the shells are not destroyed by mechanical shell milling procedure. This study has shown that carotenoid signal can not only be detected by RRS only in the native samples, but it can also be tracked through further processing steps of the material, thereby facilitating the resulting material characterization and description of the effects of a particular processing step. Hence, in following the goal of the Thesis, the usefulness of the carotenoid Raman signal in marine biotechnology research is enhanced.

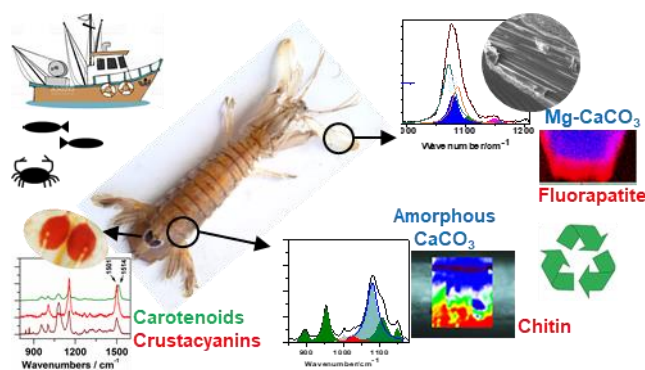
5.5. Promoting hidden natural design templates in wasted shells of the mantis shrimp into valuable biogenic composite

- *Poster presentation of the preliminary results at the 16th Confocal Raman Imaging Symposium, Ulm (Germany), 23rd - 25th September 2019*
 - Citation: Nekvapil, F., Cintă Pinzaru, S., Glamuzina, B. Hidden smart templates for blue bioeconomy: complex functional structures of marine invertebrates revealed by confocal Raman imaging. In: Book of Abstracts of the 16th Confocal Raman Imaging Symposium, WiTec GmbH, Ulm, 23rd - 25th September 2019, p. 61.

- *full-length manuscript under Minor revision for Spectrochimica Acta, Part A: Molecular and Biomolecular Spectroscopy, on 20. July 2020*

Following the successful application of Raman spectroscopy and electron microscopy techniques to identify the Atlantic blue crab (*C. sapidus*) and the

Mediterranean green crab (*C. aestuarii*) as a novel raw material, we further extend this sustainability research to a shrimp species - the mantis shrimp, *Squilla mantis*. The cuticle of this species presents an interesting combination of carbonate and phosphate biominerals. However, more importantly, carotenoids were not found all over the shrimp body, as was the case with crabs, but they were localized on the tail segment of the shrimp's body. Organization of the pigment in distinct patterns may have a biological and an ecological role. The different anatomical parts of the cuticle feature strikingly different composition in terms of biomineral and organic fraction, and the carotenoid content, as revealed by micro-Raman analysis. Hence, we propose the differential recycling of the (wasted) cuticle parts, relative to their specific composition. By publishing these results, we will advance the applicability of Raman spectroscopy techniques further into the mainstream research in the service of bioeconomy and circular economy concepts.



Graphical abstract

5.6. Chapter 5 conclusions

Important aspects on the application of Raman spectroscopy for the study of invertebrate shell pigments can be pointed out:

- chemical origin of the shell colour is due to the pigments: unsaturated polyenes, carotenoids and carotenoproteins. Crustacean shells contain carotenoids and carotenoproteins
- all the 3 pigment types of pigments are based on the conjugated polyene chain (-C=C-); however, they are spectrally distinct relative to free carotenoids: unsaturated polyenes have a reduced ν_3 band intensity or no ν_3 (C-CH) band at all (due to the lack of polyene chain methylation), while carotenoproteins exhibit a downshifted ν_1 (C=C) by about 15 to 25 cm^{-1} , and increased ν_4 intensity (due to non-covalent bonding to proteins and presumably polyene chain conformation distortion)

- differentiation between free carotenoids and those non-covalently bonded in protein carriers (e.g. astaxanthin and crustacyanin) can effectively be achieved by Lorentzian multi-peaks fitting of the ν_1 band, or by Resonance Raman spectroscopy using two excitation wavelengths (in green range for carotenoids, in red range for carotenoproteins)
- the distinctive carotenoid and carotenoprotein RRS signal can also serve as a sensitive molecular marker in powdered shells, indicating the integrity of the sensitive organic compounds

Scanning electron microscopy on native shell cross-sections also revealed differential nanoporosity of the biogenic CaCO_3 specific to each shell colour appearance. Thus, the porous shell nanoarchitecture acts as a natural supergrating, giving rise to the structural colour component.

6. CONCLUSIONS, IMPACT AND PERSPECTIVES

Carotenoids have a notable scientific and commercial value, due to their properties outlined in Section 1.2. While carotenoids can be synthesized artificially, the lab-produced analogues often do not exhibit the same properties as the natural carotenoids, the synthesis is expensive and not readily scalable, and finally, the consumer preference leans towards carotenoids from natural sources (Lindequist, 2016).

On the other hand, due to their high Raman scattering activity, carotenoids are also a useful biochemical marker, as demonstrated in Sections 5.4. and 5.5. Hence, the carotenoids will play a significant role in the further development and diversification of the scope of the Blue bioeconomy, and the entities which already work in the development of analytical methods for carotenoids may have the competitive advantage in the near future.

This Thesis comprised several lines of investigation with different experimental approach, with their specific conclusions. Nonetheless, the main theme throughout all of the described studies is the innovative way in which Raman spectroscopy tools were used to address the underlying problems of marine biophysics and environmental research from a still unconventional, but feasible, perspective. By achieving specific findings, we arm the interdisciplinary biophysics-marine biology research with new know-hows in tackling the molecular detection problems and novel potential concepts for environmental monitoring.

This Thesis demonstrated that Raman spectroscopy techniques indeed perform well in detection of carotenoid signal in marine biology/biotechnology research, with the ability to analyse native samples in a wide range of sizes and states. Several general conclusions can be made based on the presented work, which increase the depth of the Raman experimental approach and results interpretation:

- Refinement of carotenoids identification can be achieved through meaningful fitting of the $\nu_1(\text{C}=\text{C})$ band with Lorentzian components (with consideration of the expected number, position and profile width of the components),
- Addition of AgNPs to the cells or tissue extracts can have the following effects: promoting SERS excitation of carotenoids, reduction of inherent sample fluorescence, or enhances the signal of adsorbed carotenoids relative to signals of solvent,
- In cases where determining the sample carotenoid profile is difficult, comparative Raman analysis of two or more similar samples is a powerful method to exploit the subtle sample-to-sample differences and literature reports to narrow down the range of considerations and reach the correct conclusion by elimination of the implausible ones,
- Comprehensive *in situ* Resonance Raman analysis of natural pigments can only be achieved by the use of multiple laser lines resonant to different pigment types; consideration of all Raman-active chromophores present in the sample is critical,
- Coupling of experimental Raman techniques with DFT calculation notably enhances the capability of vibrational studies of carotenoids,
- Coupling of *in situ* Raman analysis with electron microscopy analysis (SEM, TEM, EDX) allows powerful structural studies.

In all of the studies Raman spectroscopy was employed as a non-destructive and direct detection method to analyse the native sample carotenoid biochemistry, without extensive preparative steps, thereby obtaining the results that represent the closest state to the natural one as possible. Furthermore, in addition to photosynthetic microorganisms and crustacean shells, which require no, or minimal, preparation, the proper and cost-effective sample preparation for Raman spectroscopy analysis was described for the case of soft tissues and extracts thereof; the best methods for particular tissues of sea urchin tissues were described in the Section 4.1.

Finally, we also deliver new insights and concrete information on biological roles and behaviour of carotenoids and, in some cases, also structural data not related to carotenoids in narrower sense, through the published articles. The concrete findings are backed up by our advanced results interpretation approaches, including band shape deconvolutions, modes intensity and area comparisons, and comparisons of spectra acquired with multiple excitation wavelengths, which allowed us to reach in-depth conclusions on sample biochemistry.

Six published original research articles and seven conference contributions are included within this Thesis. The experimental work also strengthened inter-institutional cooperation of the Faculty of Physics, Babeş-Bolyai University with the Department for Aquaculture, University of Dubrovnik and with the National Institute

for Research and Development of Isotopic and Molecular Technologies in Cluj-Napoca.

Selected references

- Abd El-Baky, H.H., El Baz, F.K., El Baroty, G.S. Evaluation of Marine Alga *Ulvalactuca* . as A Source of Natural Preservative Ingredient. *American-Eurasian J. Agric. Environ. Sci.* 2008, 3: 434-444.
- Andrei, S., Pinteau, A., Bolos, F., Bunea, A. Comparative studies regarding antioxidant actions of oxygenated normal and retro carotenoids in mouse liver and skin. *Bulletin USAMV-CN* 2007, 64: 31-35. DOI: 10.15835/buasvmcn-vm:64:1-2:2273.
- Casazza, G., Mazzella, L. Photosynthetic pigment composition of marine angiosperms: preliminary characterization of Mediterranean seagrasses. *Bul. Mar. Sci.* 2002, 7: 1171-1181.
- Chew, B.P., Park, J.S. Carotenoid action on the immune response. *J. Nutr.* 2004, 134(1): 257S–261S. DOI: 10.1093/jn/134.1.257S.
- Cintă Pinzaru, S., Müller, Cs., Tomšić, S., Venter, M.M., Cozar, B.I., Glamuzina, B. New SERS feature of β -carotene: consequences for quantitative SERS analysis. *J. Raman Spectrosc.* 2015, 46: 597-604. DOI: 10.1002/jrs.4713.
- Cintă Pinzaru, S., Müller, Cs., Tomšić, S., Venter, M.M., Brazestean, I., Ljubimir, S., Glamuzina, B. Live diatoms facing Ag nanoparticles: surface enhanced Raman scattering of bulk *Cylindrotheca closterium* pennate diatoms and of the single cells. *RSC Adv.* 2016a, 6: 42899. DOI: 10.1039/C6RA04255D.
- Cintă Pinzaru, S., Müller, Cs., Brezestean, I., Barchewitz, D., Glamuzina, B. Cyanobacteria detection and Raman spectroscopy characterization with a highly sensitive, high resolution fiber optic portable Raman system. *Studia UBB Physica* 2016b, 61: 99-108.
- Czamara, K., Majzner, K., Pacia, M.Z., Kochan, K., Kaczor, A., Baranska, M., Raman spectroscopy of lipids: a review. *J. Raman Spectrosc.* 2014, 46: 4–20. DOI: : 10.1002/jrs.4607.
- di Bernardo, M., di Carlo, M. Chapter 6: The Sea Urchin Embryo: A Model for Studying Molecular Mechanisms Involved in Human Diseases and for Testing Bioactive Compounds. in: Agnello, M. (Ed.) *Sea Urchin - From Environment to Aquaculture and Biomedicine*. InTech, London, 2017. DOI: 10.5772/intechopen.70301.
- Dose, J., Matsugo, S., Yokokawa, H., Koshida, Y., Okazaki, S., Seidel, U., Eggersdorfer, M., Rimbach, G., Esatbeyoglu, T. Free radical scavenging and cellular antioxidant properties of astaxanthin. *Int. J. Mol. Sci.* 2016, 17: 103. DOI: 10.3390/ijms17010103.
- Flores-Hidalgo, M., Torres-Rivas, F., Monzon-Bensojo, J., Escobedo-Bretado, M., Glossman-Mitnik, D., Barraza-Jimenez, D. Electronic Structure of Carotenoids in

- Natural and Artificial Photosynthesis. In: Cvetkovic, D.J., Nikolic, G.S. (eds.) Carotenoids. In: *trchOpen*, 2017 pages Chapter DOI: 10.5772/67636.
- Gundermann, K., Büchel, C. Structure and functional heterogeneity of fucoxanthin-chlorophyll proteins. In diatoms. In *The Structural Basis of Biological Energy Generation*; Hohmann-Marriott, M. F., Ed.; Springer Science+Business Media: Dordrecht, Netherlands, 2014; pp. 21-37.
- Hedegaard, C., Bardeau, J-F., Chateigner, D. Molluscan shell pigments: an in situ Resonance Raman study. *J. Molluscan Studies* 2006, 73: 157-162. DOI: 10.1093/mollus/eyi062.
- Landrum, J.T. Carotenoids: Physical, Chemical and Biological Functions and Properties. CRC Press, 2010; 568 pages
- Lindequist, U. Marine-derived pharmaceuticals – challenges and opportunities. *Biomol. Ther.* 2016, 24: 561-571; DOI: 10.4062/biomolther.2016.181.
- Maoka, T. Carotenoids as natural functional pigments. *J. Nat. Med.* 2020, 74: 1-16. DOI: 10.1007/s11418-019-01364-x.
- McBride, S.C., Price, R.J., Tom, P.D., Lawrence, J.M. Comparison of gonad quality factors: Color, hardness and resilience, of *Strongylocentrotus franciscanus* between sea urchins fed prepared feed or algal diets and sea urchins harvested from the Northern California fishery. *Aquaculture* 2004, 233: 405-422. DOI: 10.1016/j.aquaculture.2003.10.014.
- Mortensen, A., Skibsted, H.L. Importance of Carotenoid Structure in Radical-Scavenging Reactions. *J. Agric. Food Chem.* 1997, 45: 2970-2977. DOI: 10.1021/jf970010s.
- Nekvapil, F., Tomšić, S., Glamuzina, B., Barbu-Tudoran, L., Brezestean, I., Cintă Pinzaru, S., Natural nanoarchitecture of blue crab (*Callinectes sapidus* Rathbun, 1896) claw studied by Raman spectroscopy and Scanning electron microscopy. In: Vladiu, R., Mandes, A., Dinca Balan, V. (eds.) Conference proceedings. Issue 17/2017, University of Ovidius Press, p. 146 – 147.
- Nekvapil, F., Brezestean, I., Barchewitz, D., Glamuzina, B., Chiş, V., Cintă Pinzaru, S. Citrus Fruits Freshness Assessment Using Raman Spectroscopy. *Food Chem.* 2018a, 242: 560-567. DOI: 10.1016/j.foodchem.2017.09.105.
- Nekvapil, F., Tomšić, S., Cintă Pinzaru, S. Comparative Raman spectroscopy study of the coelomic fluid of grazing sea urchins and their native seawater: prospect for a potential indicator of environmental aggression. In: Şerban, G., Bătinaş, R., Tudose, T., Horváth, Cs., Croitoru, A., Holobăcă, J. (eds.) Air and water components of the environment. University Press, Cluj-Napoca, ISSN: 2067-743. 2018b, p. 27 – 34.
- Nekvapil, F., Brezeştean, I., Tomšić, S., Müller, Cs., Chiş, V., Cintă Pinzaru, S. Microsphere packages of carotenoids: intact sea urchin eggs tracked by Raman spectroscopy tools. *Photochem. Photobiol. Sci.* 2019a, 18: 1933-1944. DOI: 10.1039/c9pp00181f.

- Nekvapil, F., Molnar Muller, Cs., Tomsic, S., Cintă Pinzaru, S. Exploring the biological protective role of carotenoids by Raman spectroscopy: mechanical stress of cells. *Studia UBB Physica* 2019b, 64: 75-82. DOI: 10.24193/subbphys.2019.08.
- Nekvapil, F., Aluas, M., Barbu-Tudoran, L., Suci, M., Bortnic, R-A, Glamuzina, B., Cintă Pinzaru, S. From Blue Bioeconomy toward Circular Economy through High-Sensitivity Analytical Research on Waste Blue Crab Shells. *Sustainable Chem. Eng.* 2019c, 7: 16820-16827. DOI: 10.1021/acssuschemeng.9b04362.
- Nekvapil, F., Bunge, A., Radu, T., Cintă Pinzaru, S, Turcu, R. Raman spectra tell us so much more: Raman features and saturation magnetization for efficient analysis of manganese zinc ferrite nanoparticles. *J. Raman Spectrosc.* 2020a, 51: 959-968. DOI: 10.1002/jrs.5852.
- Nekvapil, F., Cintă Pinzaru, S., Barbu-Tudoran, L., Suci, M., Glamuzina, B., Tamaş, T., Chiş, V. Color-specific porosity in double pigmented natural 3d-nanoarchitectures of blue crab shell. *Sci. Rep.* 2020b, 10: 3019. DOI: 10.1038/s41598-020-60031-4.
- Pasteris, J.D., Wopenka, B., Freeman, J.J., Brewer, P.G., White, S.N., Peltzer, E.T., Malby, G.E. Raman Spectroscopy in the Deep Ocean: Successes and Challenges. *Appl. Spectrosc.* 2004, 58: 195A-208A. DOI: 10.1366/0003702041389319.
- Premvardhan, L., Bordes, L., Beer, A., Büchel, C., Robert, B. Carotenoid structures and environments in trimeric and oligomeric fucoxanthin chlorophyll a/c2 proteins from resonance Raman spectroscopy. *J. Phys. Chem. B* 2009, 113: 12565-12574. DOI: 10.1021/jp903029g.
- Raman, C.V. The molecular scattering of light. Nobel Prize lecture; URL: <https://www.nobelprize.org/uploads/2018/06/raman-lecture.pdf> (accessed 19. Jun 2020).
- Rygula, A., Majzner, K., Marzec, K.M., Kaczor, A., Pilarczyk, M., Baranska, M. Raman spectroscopy of proteins: a review. *J. Raman Spectrosc.* 2013, 44: 1061-1076. DOI: 10.1002/jrs.4335.
- Salares, V.R., Young, N.M., Bernstein, H.J., Carey, P.R. Resonance Raman Spectra of Lobster Shell Carotenoproteins and a Model Astaxanthin Aggregate. A Possible Photobiological Function for the Yellow Protein. *Biochemistry*, 1977, 16:4751-4756. DOI: 10.1021/bi00640a034.
- Salares, V.R., Young, N.M., Bernstein, H.J., Carey, P.R. Mechanisms of spectral shifts in lobster carotenoproteins The resonance raman spectra of ooverdin and the crustacyanins. *BBA Protein Struct.* 1979, 576: 176-191. DOI: 10.1016/0005-2795(79)90496-3.
- Sefc, K.M., Brown, A.C., Clotfelter, E.D. Carotenoid-based coloration in cichlid fishes. *Comp. Biochem. Physiol. A* 2014, 173: 42-51. DOI: 10.1016/j.cbpa.2014.03.006.
- Smith, E., Dent, G. *Modern Raman Spectroscopy - A Modern Approach*. John Wiley & Sons, Ltd. 2005; 225 pages.

Takaichi, S. Carotenoids in Algae: Distribution, Biosyntheses and Functions. *Mar. Drugs* 2011, 9: 1101-1118. DOI: 10.3390/md9061101.

Web of Science, Clarivate Analytics. URL: www.webofknowledge.com

Widjaja-Adhi., M.A.K., Ramkumar, S., von Lintig, J. Protective role of carotenoids in the visual cycle. *FASEB J.* 2018, 32: 6305-6315. DOI: 10.1096/fj.201800467R.

Zhang, X., Kirkwood, W.J., Walz, P.M., Peltzer, E.T., Brewer, P.G. A Review of Advances in Deep-Ocean Raman Spectroscopy. *Appl. Spectrosc.* 2012, 66: 237-249. DOI: 10.1366/11-06539.

Abbreviations:

AgNPs colloidal plasmonic silver nanoparticles

BBU - Babeş - Bolyai University

DFT - Density Functional Theory

EC - European Commission

EDX - electron-dispersive x-ray spectroscopy

EPS - extracellular polymeric substance

EU - European Union

FT-Raman - Fourier transform infrared Raman spectroscopy

FWHM - full width at half-maximum

IR - infrared

NA - numerical aperture

NIR - near infrared

NPs - nanoparticles

SEM - scanning electron microscopy

RS - Raman spectroscopy

RRS - Resonance Raman spectroscopy

SERS - Surface-enhanced Raman scattering

SERRS - Surface-enhanced resonance Raman scattering

TEM - transmission electron microscopy

UN - United Nations

UV - ultraviolet

Vis - visible (excitation, radiation,...)

XRPD - x-ray powder diffraction

List of publications included in the Thesis:

Original research articles

1. Citrus fruit freshness assessment using Raman spectroscopy, by Nekvapil, F., Brezestean, I., Barchewitz, D., Glamuzina, B., Chis, V., Cintă Pinzaru, S.

2. Raman spectra tell us so much more: Raman features and saturation magnetization for efficient analysis of manganese zinc ferrite nanoparticles - original research article, by Nekvapil, F., Bunge, A., Radu, T., Cinta Pinzaru, S, Turcu, R.
3. Microsphere packages of carotenoids: intact sea urchin eggs tracked by Raman spectroscopy tools, by Nekvapil, F., Brezeştean, I., Tomšić, S., Müller, Cs., Chiş, V., Cintă Pinzaru, S.
4. Exploring the biological protective role of carotenoids by Raman spectroscopy: mechanical stress of cells, by Nekvapil, F., Molnar Muller, Cs., Tomsic, S., Cintă Pinzaru, S.
5. Color-specific porosity in double pigmented natural 3d-nanoarchitectures of blue crab shell, by Citation: Nekvapil, F., Cintă Pinzaru, S., Barbu-Tudoran, L., Suci, M., Tamas, T., Chis, V.
6. From Blue bioeconomy toward Circular economy through high-sensitivity analytical research on waste Blue crab shells, by Nekvapil, F., Aluas, M., Barbu-Tudoran, L., Suci, M., Bortnic, R-A, Glamuzina, B., Cintă Pinzaru, S.

Conference contributions:

1. Are the market citrus fresh? Raman spectroscopy can promptly tell it (2017), by Nekvapil, F., Brezestean, I., Barchewitz, D., Glamuzina, B., Chis, V., Cintă Pinzaru, S., Andronie, L.
2. Raman spectroscopy analysis of metal-ferrite nanoparticles: towards precise interpretation and extraction of structural information (2019), by 1. Nekvapil, F., Bunge, A., Radu, T., Cinta Pinzaru, S., Turcu, R.
3. Raman spectroscopy in carotenoids metabolic pathways research: the example of sea urchins, by Nekvapil, F., Tomšić, S., Chiş, V., Cintă Pinzaru, S.
4. Comparative Raman spectroscopy study of the coelomic fluid of grazing sea urchins and their native seawater: prospect for a potential indicator of environmental aggression (2018), by Nekvapil, F., Tomšić, S., Cintă Pinzaru, S.
5. Rapid and cost effective tracking carotenoids in native sea urchin eggs by mullti-laser Raman spectroscopy (2018), by Nekvapil, F., Brezeştean, I., Tomsic, S., Muller, Cs., Chis, V., Cintă Pinzaru, S.
6. Natural nanoarchitecture of blue crab (*Callinectes sapidus* Rathbun, 1896) claw studied by Raman spectroscopy and Scanning electron microscopy (2017), by Nekvapil, F., Tomšić, S., Glamuzina, B., Barbu-Tudoran, L., Brezestean, I., Cintă Pinzaru, S.
7. Hidden smart templates for blue bioeconomy: complex functional structures of marine invertebrates revealed by confocal Raman imaging (2019), by 2. Nekvapil, F., Cinta Pinzaru, S., Glamuzina, B.

Summary (refers to the full-length Thesis)

- Number the pages: Main thesis (214) + Annexes (66) = 280
- Number of Annexes: 3
- Number of references used in this thesis (simple sum): 311
** Note: some references repeat in different chapters, and included published articles may contain additional references*

Number of published articles within the topic of the Thesis:

- ISI papers published: 5
- “RED” publications (Q1) as of date of publication: 4
- “YELLOW” publications (Q2) as of date of publication: 1
- Article Influence Score (AIS): 4.9

Cumulative publications:

- Accumulated AIS: 5.3
- Number of publications in conference proceedings: 15
- Number of given oral presentations: 8
- Number of created posters: 3